EXPERIMENTAL VALIDATION OF ANALYTICAL MODEL OF ONE-DIMENSIONAL CONSOLIDATION OF MULTIPLE LAYERED CLAYEY SOILS

BY

OGUNLAYI, Ayodele Joseph
MEng/SIPET/2018/9241

DEPARTMENT OF CIVIL ENGINEERING

FEDERAL UNIVERSITY OF TECHNOLOGY, MINNA

APRIL, 2023

EXPERIMENTAL VALIDATION OF ANALYTICAL MODEL OF ONE-DIMENSIONAL CONSOLIDATION OF MULTIPLE LAYERED CLAYEY SOILS

BY

OGUNLAYI, Ayodele Joseph
MEng/SIPET/2018/9241

A THESIS SUBMITTED TO THE POSTGRADUATE SCHOOL FEDERAL UNIVERSITY OF TECHNOLOGY, MINNA, NIGERIA IN PARTIAL FULFILMENT OF THE REQUIREMENTS FOR THE AWARD OF THE DEGREE OF MASTER OF ENGINEERING IN CIVIL ENGINEERING (HIGHWAY AND TRANSPORTATION ENGINEERING)

APRIL, 2023

ABSTRACT

In the field of engineering, the important of consolidation test is to determine the compressibility properties of soil for the purpose of estimating the rate of settlement and its effect on engineering structures. Over the year, a lot of analytical model have been developed to provide solution for consolidation problem in multiple layered clayey soil, most of which are still under validation process thus, given the need for this research aimed at validating and showing the extends at which the analytical model under review correspond accurately in solving a real-life consolidation problem in multiple layered clayey soil. An index and consolidation property of the soil samples was investigated for the purpose of validating the analytical model under review. Two undisturbed clayey soil sample were extracted from different locations combined to form a two layered soil element with different engineering properties. Laboratory investigation was conducted to determine their individual plastic limit, liquid limit, moisture content and particle size distribution. Oedometer test was also conducted by subjecting the soil element to consolidation procedure under a double drainage condition. Using Taylor's square root of time method, Coefficient of consolidation c_v = (5.46 x 10^{-6} m^2/min, 6.81 x 10^{-6} m^2/min), was determine from the oedometer test result and the subsequent compressibility coefficient m_v = (3.05 x 10^{-4} m^2/kN, 1.66 x 10^{-4} m^2/kN) and permeability coefficient k = (1.64 x 10^{-8} m/min, 1.11 x 10^{-8} m/min) was determine from the effective load and void ration relationship. These results were substituted into the analytical model to calculate the dissipation of excess pore water pressure u, plotted against time t, at different layer and variation of excess pore water pressure curve was generated. Experimental data are presented to show the validating of the analytical model under review.

TABLE OF CONTENTS

LIST OF TABLES

LIST OF FIGURES

APPENDICES

Appendix A **Page**

Appendix B

Appendix C

CHAPTER ONE

1.0 INTRODUCTION

1.1 Background to the Study

The important and main purpose of consolidation test on soil samples is to determine the compressibility properties of a saturated soil for estimating the rate of settlement of engineering structures according to Murthy (2007). Over the years, a lot of analytical and mathematical model have been developed to provide solutions to consolidation problem of compressible soft soil. These solutions have provided methods for the design and construction of engineering structures on various kinds of soils. In practice, the rate of consolidation in usually calculated based on Terzaghi (1925) one-dimensional consolidation theory assuming coefficient of consolidation to be constant. Consolidation due to application of instantaneous loading was studied by (Linchang. *et al.,* 2008). This theory was later corrected to consider three-dimensional effects of consolidation by Skempton and Bjerrum (1957). Olson (1977) developed a mathematical model for one-dimensional consolidation of a single layered soil profile under a simple ramp loading which does not consider the multi-layered nature of some clay profile.

Terzaghi (1943) was the first to develop a mathematical model for the rate of consolidation based on the assumption that the rate of settlement is directly related to the rate of dissipation of excess water pressure with permeability and compressibility coefficient being constant during consolidation process. This theory later became the most popular consolidation theory but with its limitations on the assumptions that consolidation of soil is a one-dimensional process, rather than three-dimensional

process. It also neglected the non-linearity and multi-layered characteristic of the soft clay.

Davis and Raymond (1965) made effort to correct some limitations of Terzaghi's theory by developing analytical solutions for different kind of one-dimensional consolidation models. This model is based on the assumptions that the decrease in permeability is proportional to the decrease in compressibility during consolidation process and the distribution of initial effective pressure is constant with depth (Kang-He, *et al*., 2002). Davis and Raymond (1965) assumed that the coefficient of consolidation, C_v remained constant as compressibility, m_v and permeability, k_v decreases with increase in pressure. Based on these assumptions, the Davis and Raymond consolidation theory become the first and more accurate consolidation theory for a non-linear compressible clay soil (Zhuang, *et al.,* 2005). Yet the multi-layered characteristics of natural soils are not adequately considered.

Guofu and Jian-Hau (2000) adopted a Finite Differential Method (FDM)) to present numerical solutions for pore water pressure and average consolidation degree. The modification of theory of one-dimensional consolidation is modified based on Non-Darcian flow produced by non-Newtonian liquid to consider the variation in the total vertical stress with depth and time. The study founded that the water flow law parameters have an important effect on the rate of consolidation and the percent of the equivalent water head of external load to the soil layer depth have a strong influence on the rate of consolidation. Also, the rate of consolidation is slow when the applying load is slow.

Kim *et al.,* (2021) concludes that analytical solutions can be more accurate and simpler comparing with numerical solutions. In addition, analytical solutions can be used for verification of numerical methods. However, due to the complexity of the nonlinear consolidation equations for multi-layered soil, none of researchers have ever derived any analytical solutions for one-dimensional nonlinear consolidation of multi-layered soil under time-dependent loading. An analytical model for one-dimensional electro-osmotic consolidation of double layered system was presented by Zhao *et al.,* (2020) as an innovative technique for ground improvement considering the heterogeneity nature of soil. An explicit solution was developed through a computer programming for excess pore pressure and degree of consolidation. To further the research into analytical solution for the consolidation of layered soils, Zhou *et al.,* (2023) developed a new concept called drainage by deriving a generalized analytical solution for unsaturated soil consolidation under partial permeable boundaries condition using Laplace transform technique. This provide a semi analytical solution of excess pore-air and excess pore water pressure and settlement of double layered unsaturated ground.

Sadiku (1991) developed a single partial differential equation for the pore pressure variation in the composite soil medium of two horizontal layers. It established a systematic analysis for consolidation problems, obtained a general equation applicable for solving a wide range boundary condition by a generalized Fourier series in terms of Eigen functions of the composite soil medium obtained from an auxiliary differential problem. It further established the algebraization of the auxiliary problem of consolidation which makes it conformable with computer applications that shows the theoretical relationship of degree of consolidation, U and time factors, T of multi-layered soils. Sadiku developed an analytical model using numerical method for solving consolidation problem of double layered soil. Thus, the following equations were

adopted for validation from Sadiku (1991), analytical model in solving multi-layered clayey soil consolidation problem.

For layer 1

$u(z,t) = \sum_{j=1}^{3} e^{-\omega_j T} \phi_j(z)$ (Sadiku 1991)

$$u(z,t) = \left\{e^{-0.0687T} v\left(0.8255\ sin\frac{\pi z}{l} - 0.3418\ sin\frac{2\pi z}{l} - 0.0471\ sin\frac{3\pi z}{l}\right)\right.$$
$$+ \quad e^{-0.2816T} v\left(0.2606\ sin\frac{\pi z}{l} + 0.6986\ sin\frac{2\pi z}{l} - 0.5491\ sin\frac{3\pi z}{l}\right)$$
$$+ \quad \left. e^{-1.6660T} v\left(0.2944\ sin\frac{\pi z}{l} + 0.5701\ sin\frac{2\pi z}{l} + 0.8155\ sin\frac{3\pi z}{l}\right)\right\} \quad (1.1)$$

At the common boundary, excess pore water pressure is given by

$$u(z,t) = \left\{e^{-0.0093t} \Omega_1\left(106.66\ sin\frac{\pi z}{l} - 44.16\ sin\frac{2\pi z}{l} - 6.09\ sin\frac{3\pi z}{l}\right)\right.$$
$$+ \quad e^{-0.0380t} \Omega_2\left(33.67\ sin\frac{\pi z}{l} + 90.26\ sin\frac{2\pi z}{l} - 70.95\ sin\frac{3\pi z}{l}\right)$$
$$+ \quad \left. e^{-0.2247t} \Omega_3\left(38.04\ sin\frac{\pi z}{l} + 73.66\ sin\frac{2\pi z}{l} + 105.37\ sin\frac{3\pi z}{l}\right)\right\} \quad (1.2)$$

For layer 2

$$u_2(z,t) = \left\{e^{-0.0687T} v\left(0.8255\ sin\frac{\pi z}{l} - 0.3418\ sin\frac{2\pi z}{l} - 0.0471\ sin\frac{3\pi z}{l}\right)\right.$$
$$+ \ e^{-0.2816T} v\left(0.2606\ sin\frac{\pi z}{l} + 0.6986\ sin\frac{2\pi z}{l} - 0.5491\ sin\frac{3\pi z}{l}\right)$$
$$+ \ \left. e^{-1.6660T} v\left(0.2944\ sin\frac{\pi z}{l} + 0.5701\ sin\frac{2\pi z}{l} + 0.8155\ sin\frac{3\pi z}{l}\right)\right\} \quad (1.3)$$

Given that

$$\Omega_{rr} = -\frac{k_1\pi}{2l}\left\{r^2\pi\left[\alpha + (1-\alpha)\left(\lambda + \frac{\sin 2r\lambda\pi}{2r\pi}\right)\right] - \psi_j\pi\left[\beta + (1-\beta)\left(\lambda - \frac{\sin 2r\lambda\pi}{2r\pi}\right)\right]\right\} \quad (1.4)$$

Where

$$\psi_j = \left(\frac{m_1\gamma_w l^2}{k_1\pi^2}\right)\omega_j, \quad (1.5)$$

$$\psi_1 = \left(\frac{3.053 \times 10^{-4} \times 9.81 \times 0.02^2}{1.64 \times 10^{-8}\pi^2}\right) 0.0687 = 0.5085$$

$$\psi_2 = \left(\frac{3.053 \times 10^{-4} \times 9.81 \times 0.02^2}{1.64 \times 10^{-8}\pi^2}\right) 0.2816 = 2.0842$$

$$\psi_3 = \left(\frac{3.053 \times 10^{-4} \times 9.81 \times 0.02^2}{1.64 \times 10^{-8}\pi^2}\right) 1.6660 = 12.3307$$

$$\propto = \frac{k_2}{k_1} = \frac{1.11 \times 10^{-8}}{1.64 \times 10^{-8}} = 6.7683 \times 10^{-17}$$

$$\beta = \frac{m_2}{m_1} = \frac{1.659 \times 10^{-4}}{3.053 \times 10^{-4}} = 5.4340 \times 10^{-9}$$

$$\lambda = \frac{h_2}{h_1} = \frac{0.01}{0.01} = 1$$

1.2 Problem Statement

In nature, the soil stratum generally consists of multi-layers due to the complex sedimentation. Under this situation, it seems to be unreasonable to treat this type of soil stratum as a homogenous one **(**Suhua *et al.*, 2021).

Consolidation problem of multi-layers soil deposit are not amenable to solution using Terzaghi's one dimensional consolidation principle of single layer clay (Sadiku 1991).

Even though noteworthy progress has been made to study the consolidation problems of layered soil, the related research is still imperfect and needs further study for its complexity (Wenbing *et al.*, 2018).

1.3 Aim and Objectives of the Study

1.3.1 Aim of the study

The aim of this study is to validate experimentally an analytical model of one-dimensional consolidation of multiple layered clayey soils.

1.3.2 Objectives of the study

The objectives of this research are to:

(i) Determine the index properties of the clayey soil sample.

(ii) Determine the consolidation properties of the clayey soil sample.

(iii) Validate the analytical model under review.

1.4 Justification of the Study

The correctness and accuracy of the derived analytical equation for the excess pore water pressure as well as degree of consolidation in multi-layered clayey soil is paramount to its acceptability in providing solution to consolidation problem in multiple layers soils.

1.5 Scope of the Study

The scope of this research is to investigate the index and consolidation properties of the clay soil samples through laboratory experiment, determine the excess pore water pressure u and validate the analytical model under review by generating the excess pore water pressure distribution curve from the analytical equation.

CHAPTER TWO

2.0 LITERATURE REWIEW

2.1 Background Information

When a soil layer is subjected to compressive stress, such as during the construction of structure, road, and runway, it will exhibit certain amount of compression. This compression of soils could be the rearrangement of the soil solids or extrusion of the pore water from the soil (Braja 1997). According to Terzaghi (1943), ‘‘a decrease of water content of a saturated soil without replacement of the water by air is termed as consolidation processes.’’ When saturated clay soils with low permeability are subjected to compressive stresses due to structural loading, the pore water will immediately increase; however, due to low permeability of the soil, there will be a time lag between the application of load and the extrusion of the pore water. This whole process is called consolidation (Braja 1997). However, this review work describes the various works on consolidation of multi-layered clayey soil analytical solution and modelling from different scholars.

2.2 Consolidation Theory

Consolidation is the process by which soil decreases in volume through dissipation of excess pore water pressure either under its own weight over time or on the application of effective stresses during construction activities. However, settlement is the prior stage of consolidation where effective stress does not exist. The knowledge of the two phenomenal is fundamental in consolidation process (Smith 1981).

Consolidation phenomenon is basically a problem of non-steady flow of water through a porous soil mass. The different between the quantity of water entering the lower surface

at a depth h, and the quantity of water that escape the upper surface at a depth h_2 in time t must be equal to the volume change of the material (Murthy 2007).

Figure 2.1 shows a layer of clay thickness H_t located below groundwater level and between two highly permeable sand layers. If a surcharge of intensity, $\Delta\sigma$ is applied at the ground surface over a very large area, the pore water pressure in the clay increases. For a surcharge of infinite extent, the immediate increase of the pore water pressure, Δu, at all depths of the clay layer is equal to the total stress $\Delta\sigma$.

Thus $\Delta u = \Delta\sigma$

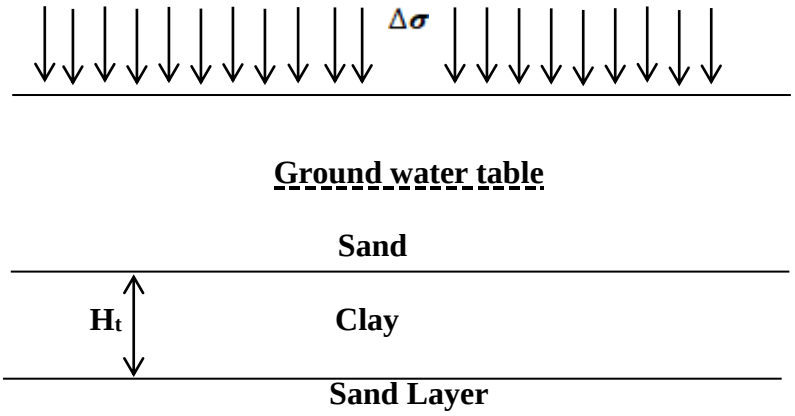

Figure. 2.1: Principle of Consolidation

However, the total stress is equal to the sum of the effective stress and the pore water pressure. At all depths of the clay layer, the increase of effective stress due to the surcharge at the instance of load application is equal to zero. Thus $\Delta\sigma' = 0$, where $\Delta\sigma'$ is the increase of effective stress. At time t = 0, the entire increase in stress at all depths of the clay is taken by the pore water pressure and none by the soil. Also, for load applied over a limited area, it may not be true that the increase of the pore water pressure is equal to the increase of vertical stress at any depth at time t = 0.

At a time, t > 0, the water in the void spaces of the clay layer will be squeezed out and will flow towards both the highly permeable sand layers, thereby reducing the excess

pore water pressure. However, the effective stress is increase by an equal amount, since $\Delta\sigma' + \Delta u = \Delta\sigma$. When t = 0, $\Delta\sigma > 0$ and $\Delta u < \Delta\sigma$

Table 2.1: Summary of the variation of $\Delta\boldsymbol{\sigma}$, $\Delta\boldsymbol{u}$ and $\Delta\boldsymbol{\sigma'}$

Time t	Total stress increase $\Delta\sigma$	Excess pore water pressure Δu	Effective stress increase $\Delta\sigma'$
0	$\Delta\sigma$	$\Delta\sigma$	0
>0	$\Delta\sigma$	$< \Delta\sigma$	>0
∞	$\Delta\sigma$	0	$\Delta\sigma$

The overall gradual process of increase in effective stress in the clay layer due to the surcharge which result in a settlement that is time–dependent, is simply know as consolidation process (Braja, 1997).

2.2.1 One-dimensional consolidation theory

The theory of one – dimensional consolidation was first proposed by Karl Terzaghi in 1927 to predict the time – rate of consolidation of a consolidating layer and the pore pressure at any elapsed time at any location in the field of geotechnical engineering. The following assumptions were made by Terzaghi during the process:

(i) The clay layer is homogeneous.

(ii) The clay layer is completely saturated.

(iii) Deformation of soils occurs only in one direction (vertical) in the direction of load application.

(iv) Darcy's law is valid.

(v) The compression of the soils layer is due to change in volume only, which in turn, is due to the squeezing out of water from the void's spaces.

(vi) The coefficient of consolidation c_v is constant.

Figure 2.2a and 2.2b show the general nature of distribution of, Δu and $\Delta\sigma'$ with depth.

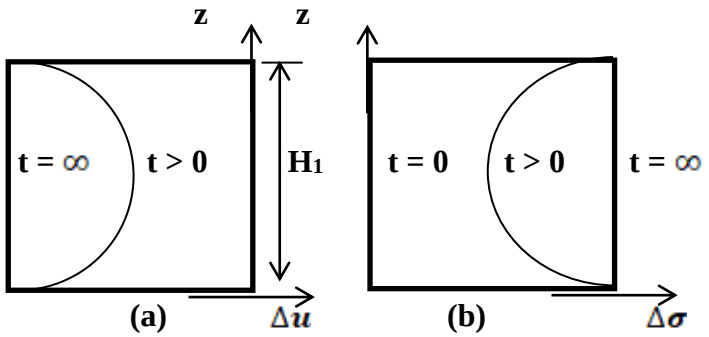

Figure 2.2: Distribution of Δu and $\Delta\sigma$

During consolidation process, flow occurs in three orthogonal directions, and the soils layer volume also change with change in the three directions. The process could be represented mathematically by continuity equation given in Eq. 2.1

$$\left(\frac{\partial v_x}{\partial x} + \frac{\partial v_y}{\partial z} + \frac{\partial v_z}{\partial z}\right) dxdydz = \frac{\partial W}{\partial t} \qquad (2.1)$$

The left-hand side of the equation represents the amount of water flowing into the soil layer in the direction of dx, dy and dz, minus the amount of water leaving the soil layer per unit time. The right-hand side represents the rate of depletion of water in the soils per unit time. However, Terzaghi assumed one dimensional consolidation situations with one dimensional flow, therefore the continuity equations are then reduced to

$$\left(\frac{\partial v_z}{\partial z}\right) dxdydz = \frac{\partial W}{\partial t} \qquad (2.2)$$

Given that Darcy's law is valid, $v_z = k_z \frac{\partial h}{\partial z}$ and soil is homogeneous, $k_z = f(z)$

Then $$\frac{\partial v_z}{\partial z} = k_z \frac{\partial^2 h}{\partial z^2} \qquad (2.2a)$$

where h is the head causing flow

Or

$$\frac{\partial v_z}{\partial z} = \frac{k_z}{\gamma_w} \frac{\partial^2 u}{\partial z^2} \qquad (2.2b)$$

Where u is the excess pore water pressure causing flow during consolidation process, h = u/γ_w assuming that $\gamma_w \neq f(z)$. Thus Eq. 2.2 can be rewrite as

$$\frac{\partial W}{\partial t} = \frac{k_z}{\gamma_w}\frac{\partial^2 u}{\partial z^2} \tag{2.3}$$

Where ∂W represent the change in volume of the soil layer in all directions and $\frac{\partial W}{\partial t} = \frac{\partial}{\partial t}$

In a soil layer of volume v equal to dx, dy, dz at an initial void ratio e_o, the volume of the voids $v_{v,} = \frac{e_o}{1+e_o}$ dxdydz. Where v_v experience changes, (e) becomes variable and $v_{v,} = \frac{e}{1+e_o}$ dxdydz.

Since the volume of soil grains does not change, but the change in volume in a soil layer is due to change in the voids volume.

$$\frac{\partial W}{\partial t} = \frac{\partial}{\partial t}(dxdydz) = \frac{\partial}{\partial t}\left(\frac{e}{1+e_o}dxdydz\right)$$

Where volume of soils grain = constant = $\frac{e}{1+e_o}dxdydz$

Then $$\frac{\partial W}{\partial t} = \frac{\partial}{\partial t}\left(\frac{e}{1+e_o}dxdydz\right) = \frac{\partial e}{\partial t}\left(\frac{dxdydz}{1+e_o}\right) \tag{2.4}$$

For a change in effective stress, $a_v = \frac{\Delta e}{\Delta \sigma}$, de = $-a_v d\bar{\sigma}$ (-ve sign as e decrease with increase in $\bar{\sigma}$). The excess pore water dissipates while the effective stress increases in consolidation process, $d\bar{\sigma}$ = -du. Thus de = $a_v$du.

Substituting for de in Eq. 2.4

$$\frac{\partial W}{\partial t} = \frac{dxdydz}{1+e_o}\frac{\partial e}{\partial t} = \frac{dxdydz}{1+e_o}a_v\frac{\partial u}{\partial t} \tag{2.5}$$

Substituting for $\frac{\partial W}{\partial t}$ of Eq. 2.5 in Eq. 2.2

$$\frac{k_z}{\gamma_w}\frac{\partial^2 u}{\partial z^2} = \frac{a_v}{1+e_o}\frac{\partial u}{\partial t} = m_v\frac{\partial u}{\partial t} \tag{2.6}$$

Where m_v = coefficient of volume compressibility = $\frac{a_v}{1+e}$ (2.7)

The coefficient of consolidation, c_v is define such that

$$\frac{\partial u}{\partial t} = \frac{k_z \partial^2 u}{\gamma_w m_v \partial z^2} = c_v \frac{\partial^2 u}{\partial z^2} \quad (2.8)$$

Where c_v = coefficient of consolidation = $\frac{k_z}{\gamma_w m_v}$ (2.9)

According to Braja (1997), Eq. 2.8 is the differential equation of consolidation. It relates to the rate of change of excess hydrostatic pressure to the rate of expulsion of excess pore water from a unit volume of soil during the same time interval. The solution to this equation is obtained by means of the Fourier Series. For the case of one-dimensional consolidation shown in Figure 2.2, the boundary condition is given bellow.

(i) At t = 0 at any distance z: u = u_i = $\Delta\sigma$ (constant)

(ii) At t = ∞ at any distance z: u = 0

(iii) At any time, t at z = 0: u = 0

(iv) At any time, t at z = H: u = 0

According to Terzaghi if u is assumed to be a product of some functions of z and t, it may be represented by the equation.

$$u(z,t) = \sum_{m=0}^{\infty} \frac{2u_0}{M} \sin\frac{Mz}{H} e^{-(M^2 Tv)} \quad (2.10)$$

The variation of Uz with depth for various values of non-dimensional time factor Tv is also given.

$$U_z = 1 - \sum_{m=0}^{\infty} \frac{2}{M} \sin\frac{Mz}{H} e^{-(M^2 Tv)} \quad (2.11)$$

2.2.2 One-dimensional nonlinear consolidation theory

The one-dimensional consolidation theory developed by Terzaghi (1925) was void of the non-linearity characteristic of a natural soil layer. Hence the needs for further researcher work to consider the non-linearity of the soil layer. Davis and Raymond (1965) developed an analytical theory which was used to correct the limitations of

Terzaghi's theory of one-dimensional consolidation which considered the non-linearity of the natural soil layer.

Davis and Raymond (1965) developed a theory of non-linear consolidation for oedometer boundary conditions assuming the coefficient of consolidation, c_v remained constant, coefficient of compressibility mv and permeability k_v varied with an increment in pressure. Thus, the following assumptions and equations were made and developed by Davis and Raymond (1965)

(i) The coefficient of compressibility, mv of a normally consolidated soil is given:

$$mv = -\frac{1}{1+e}\frac{\partial e}{\partial \sigma'} \quad (2.12)$$

where e = void ratio and σ' = effective pressure.

(ii) Result of oedometer tests on normally consolidated soil have shown that the empirical law $e = e_o - I_c \log_{10}\frac{\sigma'}{\sigma_o'}$ (2.13)

where e_o = void ratio of soil subject to pressureσ_o', σ_o' is effective pressure at point 'o' on the e-logσ' curve, and I_c is compression index of soil assumed constant. Differentiating void ratio e, with respect to effective pressure and substituting in equation. 2.31 gives:

$$m_v = \frac{0.434\, I_c}{(1+e)\sigma'} \quad (2.14)$$

(iii) During consolidation process, (1+e) varies with time far less than the effective pressure σ' so that (1+e) may be considered constant for any load. Thus Eq. 2.3 becomes

$$m_v = \frac{A}{\sigma'} \quad (2.15)$$

where A = constant

(iv) Result of oedometer tests on normally consolidated soils show that coefficient of consolidation c_v varies much less than the coefficient of compressibility mv and may be taken as relatively constant. Hence the assumption.

$$c_v = \frac{k}{m_v \gamma_w} \tag{2.16}$$

where k = permeability of the soil and γ_w = bulk density of water.

(v) The soil is laterally confined.

(vi) Total stresses are the same, effective stresses are the same for every point on a horizontal layer.

(vii) Darcy's law is valid and applicable to the movement of water through the soil.

Thus $v = ki = \frac{k}{\gamma_w}\frac{\partial u}{\partial z}$ (2.17)

where v = velocity of flow, i= hydraulic gradient, k = coefficient of permeability, u = excess pore water pressure, and z = height above the impermeable boundary. The rate of water lost per unit area in a small element of soil thickness dz. $\frac{\partial v}{\partial z}dz = \frac{\partial}{\partial z}\left(-\frac{k}{\gamma_w}\frac{\partial u}{\partial z}\right)dz$

Substituting Eq. (2.14) and Eq. (2.15) gives

$$\frac{\partial v}{\partial z}dz = -\frac{\partial}{\partial z}\left(m_v c_v \frac{\partial u}{\partial z}\right)dz = -\frac{\partial}{\partial z}\left(\frac{Ac_v}{\sigma'}.\frac{\partial u}{\partial z}\right)dz$$

$$= -Ac_v\left[\frac{1}{\sigma'}.\frac{\partial^2 u}{\partial z^2} - \left(\frac{1}{\sigma'}\right)^2 \frac{\partial u}{\partial z}.\frac{\partial \sigma'}{\partial z}\right]dz \tag{2.18}$$

(viii) The soil is completely saturated; pore water pressure and soil particles are incompressible relative to the soil layer. Therefore,

$$\sigma = \sigma' + u \tag{2.19}$$

where σ is total pressure. Differentiating with respect to depth gives:

$$\frac{\partial \sigma}{\partial z} = \frac{\partial \sigma'}{\partial z} + \frac{\partial u}{\partial z} \tag{2.20}$$

if total stress is constant with depth, then

$$\frac{\partial \sigma}{\partial z} = 0 \tag{2.21}$$

(ix) Secondary consolidation is ignored.

(x) The strain developed within the soil element is giving:

$$f = \frac{e_n - e}{1+e_n} = \frac{I_c}{1+e_n} \log_{10} \frac{\sigma'}{\sigma'_n} \tag{2.22}$$

where f is strain and the void ratio corresponding to zero strain and to the stress σ'_n. Differentiating strain with respect to time to obtain the rate of water lost per unit area:

$$\frac{\partial f}{\partial t} = \frac{I_c}{1+e_n} \cdot \frac{0.434}{\sigma'} \cdot \frac{\partial \sigma'}{\partial t} \tag{2.23}$$

Where t is time, assuming that (1+en) is approximately equal to (1+e) in Eq. (2.12) and Eq. (2.13):

$$\frac{\partial f}{\partial t} = \frac{A}{\sigma'} \cdot \frac{\partial \sigma'}{\partial t} \tag{2.24}$$

Substituting Eq. 2.16 and Eq. 2.22 gives:

$$-c_v \left[\frac{1}{\sigma'} \cdot \frac{\partial^2 u}{\partial z^2} - \left(\frac{1}{\sigma'} \right)^2 \frac{\partial u}{\partial z} \cdot \frac{\partial \sigma'}{\partial z} \right] = \frac{1}{\sigma'} \cdot \frac{\partial \sigma'}{\partial t} \tag{2.25}$$

Equation 2.23 becomes the general equation for non-linear consolidation of clay soil.

2.3 Consolidation of Double-layered Soil

Terzaghi (1943) proposed his consolidation theory and the principle of effective pressure for one-dimensional consolidation neglected the nonlinearity of soil for practical purposes. Davis and Raymond (1965) started from where Terzaghi stopped by deriving an analytical solution for the constant loading case on nonlinear consolidation of single layer soil and on the assumptions that the decrease in permeability is proportional to the decrease in compressibility during consolidation process neglecting the layered characteristics of natural soils.

However, the soils as it is in nature are often layered and it is unrealistic to assume that the soil strata are single soil layer. In recent time, researchers have been more concerned on consolidation problems of double layered soil and work has greatly increased in the recent year. Schiffman and Stein (1970) developed a solution for multi-layered consolidation problem under depth-independent loading. Tang and Onitsuka (2001) introduced vertical drain to accelerate the consolidation process, with the assumptions that the total load remains constant during consolidation. Miao *et al.,* (2008) presented an analytical solution for consolidation of a double-layered compressible foundation partially penetrated by deep mixed columns.

Kim *et* al., (2021) presented an analytical solution for the one-dimensional nonlinear consolidation of double-layered soil associated with time-dependent loading based on the work of Davis and Raymond (1965). More recently, Junhui *et al.,* (2015) further investigated the consolidation problems of multi-layered soil for different engineering conditions. Even though noteworthy progress has been made to study the consolidation problems of layered soil, the related research is still imperfect and needs further study for its complexity (Wenbing *et al.,* 2018). Miao *et al.,* (2008) presented a double layered consolidation analytical solution for embankment constructed on footing moderately imbedded penetrated by deep mixed columns, one way and two-way drainage are conducted. The calculation of time-settlement relationship used consolidation algorithm. Laplace method of transformation was adopted to solve the consolidation equations and Stehfest algorithm was adopted to explain the inverse Laplace transform for time-dependent loading. Two stage of loading describes an effect of the first loading time on the consolidation degree of the system. The study shows that

for the double layered soil system; the stiffness has a significant role in the consolidation role and the hard soil exhibit faster rate of consolidation (Tawfek, 2017).

Braja (2019), presented a numerical solution in the calculations of excess pore water pressure at the interface of two different types of clayey soil having different value of coefficient of consolidation cv and permeability k, by the modification of Eq. 2.26.

$$\frac{k}{c_v}\frac{\partial u}{\partial t} = k\frac{\partial^2 u}{\partial z^2}$$

$$k\frac{\partial^2 u}{\partial z^2} = \frac{1}{2}\left[\frac{k_1}{(\Delta z)^2} + \frac{k_2}{(\Delta z)^2}\right]\left(\frac{2k_1}{k_1+k_2}\,u_{1,t} + \frac{2k_2}{k_1+k_2}\,u_{3,t} - 2u_{0,t}\right) \quad (2.26)$$

Where k_1 and k_1 are the coefficient of permeability in layer 1 and 2 respectively. $u_{1,t}$, $u_{1,t}$ and $u_{1,t}$ are the excess pore water pressure at time t for point 0, 1, and 3 respectively as shown in Figure 2.3b

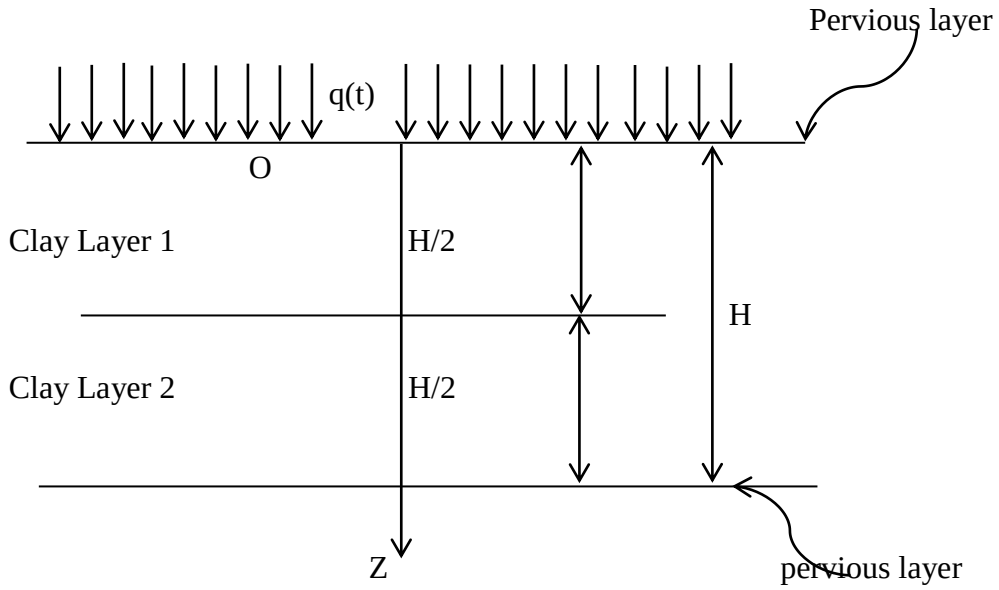

(a)

Figure 2.3a: Double layered clay soil

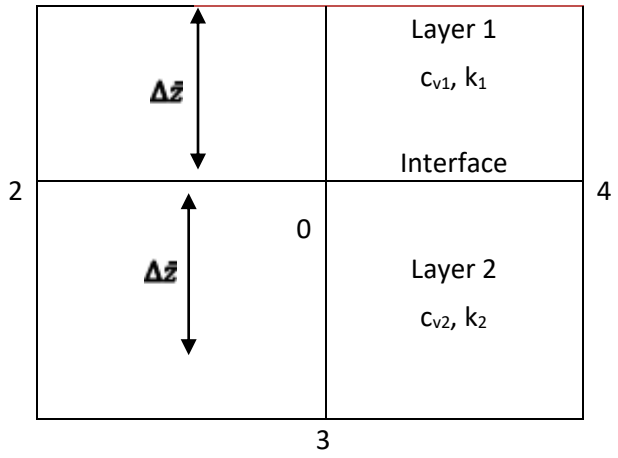

(b)

Figure 2.3b: Double layered clay soil

The average volume change for the soil element at the boundary is given as;

$$\frac{k}{c_v}\frac{\partial u}{\partial t} = \frac{1}{2}\left[\frac{k_1}{c_{v1}} + \frac{k_2}{c_{v2}}\right]\frac{1}{\Delta t}\left(u_{0,t+\Delta t} - u_{0,t}\right) \quad (2.27)$$

Where $u_{0,t}$ and $u_{0,t+\Delta t}$ are the excess pore water pressure at point 0, at time t+Δt respectively. Equating the right-hand side of Eq. (2.25) and (2.25)

$$\left[\frac{k_1}{c_{v1}} + \frac{k_2}{c_{v2}}\right]\frac{1}{\Delta t}\left(u_{0,t+\Delta t} - u_{0,t}\right) = \frac{1}{(\Delta z)^2}(k_1 + k_2)\left(\frac{2k_1}{k_1+k_2}u_{1,t} + \frac{2k_2}{k_1+k_2}u_{3,t} - 2u_{0,t}\right) \quad \text{Or}$$

$$u_{0,t+\Delta t} = \frac{\Delta t c_{v1}}{(\Delta z)^2} \text{ x } \frac{1+k_2/k_1}{1+\left(\frac{k_2}{k_1}\right)\left(\frac{c_{v1}}{c_{v2}}\right)} \text{ x } \left(\frac{2k_1}{k_1+k_2}u_{1,t} + \frac{2k_2}{k_1+k_2}u_{3,t} - 2u_{0,t}\right) + u_{0,t} \quad (2.28)$$

Assuming $\frac{1}{t_R} = \frac{c_{v1}}{z_R^2}$

Therefore,

$$\bar{u}_{0,t`+\Delta t`} = \frac{\Delta t`}{(\Delta z`)^2} \text{ x } \frac{1+k_2/k_1}{1+\left(\frac{k_2}{k_1}\right)\left(\frac{c_{v1}}{c_{v2}}\right)} \text{ x } \left(\frac{2k_1}{k_1+k_2}\bar{u}_{1,t`} + \frac{2k_2}{k_1+k_2}\bar{u}_{3,t`} - 2\bar{u}_{0,t`}\right) + \bar{u}_{0,t`} \quad (2.29)$$

Sadiku (1991), presented a systematic approach for the analytical solutions to consolidation problems of multi-layered soil through a rigorous analysis of the problem to form an expression for the solution by way of a generalized Fourier series to obtain a wide range practicable boundary condition. The eigenfunctions of the composite

medium are the coordinate functions of the series, obtained computationally through the application of the extended equations of Galerkin (Sadiku, 2013). For practical purposes, this analysis was based on the Figure 2.3a; two layers of different compressibility undergoing simultaneous consolidation. In agreement with Terzaghi's theory of one-dimensional consolidation, the space time variations of pore pressure in the layers are given by:

$$k_1 = \frac{\partial^2 u_1}{\partial z^2} = m_1 \gamma_w \frac{\partial u_1}{\partial t}; \qquad 0 \leq z \leq h_1 \tag{2.30}$$

$$k_2 = \frac{\partial^2 u_2}{\partial z^2} = m_2 \gamma_w \frac{\partial u_2}{\partial t}; \qquad h_1 \leq z \leq H \tag{2.31}$$

Where u, k, and m are the soil pore pressure, the permeability coefficient and the compressibility coefficient respectively, γ_w=unit weight of water, t = time and the subscripts 1, 2 refers to the appropriate layers. The excess pore water pressure is given by;

$$u(z,t) = \begin{cases} u_1 & if\ 0 \leq z \leq h_1 \\ u_2 & if\ h_1 \leq z \leq H \end{cases}$$

Sadiku (1991) presented the Laplace image of u(z, t) as shown in the equation below:

$$\bar{u}(z,s) = \sum_{j=1}^{\infty} \frac{\phi_j(z)}{\omega j + s} \int_0^1 \rho(\xi)\phi_j(\xi)q(\xi)d\xi \tag{2.32}$$

Performing an Inverse Laplace transformation on Eq. (2.30) to provide a solution equation to the problem presented by Sadiku (1991) gives the following.

$$u(z,t) = \sum_{j=1}^{\infty} e^{-\omega t} \int_0^1 \rho(\xi)\ \phi_j(z)\ \phi_j(\xi)\ q(\xi)d\xi \tag{2.33}$$

Thus, $\phi_j(z)$ is expressed as a finite linear combination of certain basic functions which satisfy all the boundary conditions of the problem. There are hardly any smooth common functions which would satisfy the external boundary conditions, in additions to which satisfy the matching conditions at the common boundary. Therefore, the Galerkin application in its classical form would be inapplicable (Sadiku, 2013).

Considering Galerkin;s approach in which drainage occurs at both top and bottom surface

$$\mu_r(z) = sin\frac{r\pi z}{H} \tag{2.34}$$

where $\mu_r(0) = 0$ and $\mu_r(H) = 0$

Hence, $\mu_r(z)$ satisfy external boundary conditions.

However, $k_1\,\mu_r(h_1) \neq k_2\,\mu_r(h_2)$ that is, the matching condition is violated.

Moreover, given that

$$\phi_j(z) = \sum_{r=1}^{N} a_{jr}\,\mu_r(z) \tag{2.35}$$

Where a_{jr} are coefficient to be determined, which lead to the Galerkin equation.

$$\sum_{r=1}^{N} a_{jr}\,\Omega_{rn} = 0$$

Where

$$\Omega_{rn} = \int_0^1 \left[\eta(z)\,\mu_r''(z) + \omega_j\rho(z)\mu_r(z)\right]\mu_n(z)dz - k_1(1-\alpha)\mu_r'(h_1)\,\mu_n(h_1) \tag{2.36}$$

r,n = 1,2,3,…N

With the rigorous mathematical analysis and algebraization of the auxiliary problem using Galerkin method and back substitution into Eq. (2.32) the corresponding values of a_{jr} are obtained.

$$\Omega_r = -\frac{k_1\pi}{2l}\left\{(1-\alpha)rn\left[\frac{sin(r-n)\lambda\pi}{(r-n)} + \frac{\sin(r-n)\lambda\pi}{(r+n)}\right] - \psi_j(1-\beta)\left[\frac{\sin(r-n)\lambda\pi}{(r-n)} - \frac{\sin(r+n)\lambda\pi}{(r+n)}\right]\right\} \tag{2.37}$$

$$\Omega_{rr} = -\frac{k_1\pi}{2l}\left\{r^2\pi\left[\alpha + (1-\alpha)\left(\lambda + \frac{\sin 2r\lambda\pi}{2\,r\pi}\right)\right] - \psi_j\pi\left[\beta + (1-\beta)\left(\lambda - \frac{\sin 2r\lambda\pi}{2r\pi}\right)\right]\right\} \tag{2.38}$$

Where $\psi_j = \left(\frac{m_1\gamma_w l^2}{k_1\pi^2}\right)\omega_j$, $\propto = \frac{k_2}{k_1}$ and $\beta = \frac{m_2}{m_1}$ and $\lambda = \frac{h_2}{h_1}$ in which $\lambda = 0.2$, $\alpha = 0.1$ and $\beta = 2.5$

The 3 term Galerkin approximation (N = 3),

$$\omega_1,\ \omega_2,\ \omega_3 = \{0.0687, 0.2816, 1.6660\}$$

The correspondence normalized Eigen functions are

$$\phi_1(z) = v\left(0.8255\ sin\frac{\pi z}{l} - 0.3418 \sin\frac{2\pi z}{l} - 0.0471 \sin\frac{3\pi z}{l}\right),$$

$$\phi_2(z) = v\left(0.2606\ sin\frac{\pi z}{l} + 0.6986 \sin\frac{2\pi z}{l} - 0.5491 \sin\frac{3\pi z}{l}\right)$$

$$\phi_3(z) = v\left(0.2944\ sin\frac{\pi z}{l} + 0.5701 \sin\frac{2\pi z}{l} + 0.8155 \sin\frac{3\pi z}{l}\right)$$

where $v = (m_1\gamma_w l)^{-1/2}$

Given the condition that the initial pore pressure is considered to be equal for all z, that is $u_o \forall z = q(z)$ where u_o is constant, then the space – time variation of u is given by:

$$\begin{aligned} u(z,t) = \Big\{ & e^{-0.0687T}\left(3.3188\ sin\frac{\pi z}{l} - 1.3740\ sin\frac{2\pi z}{l} - 0.1892\ sin\frac{3\pi z}{l}\right) + \\ & e^{-0.2816T}\left(0.0809\ sin\frac{\pi z}{l} + 0.2168\ sin\frac{2\pi z}{l} - 0.1704\ sin\frac{3\pi z}{l}\right) + \\ & e^{-1.6660T}\left(0.5646\ sin\frac{\pi z}{l} + 1.0932\ sin\frac{2\pi z}{l} - 1.5639\ sin\frac{3\pi z}{l}\right)\Big\} \end{aligned} \quad (2.39)$$

Or

$$u(z,t) = \sum_{j=1}^{3} e^{-\omega_j T}\phi_j \quad (2.40)$$

Where *T* is the dimensionless quantity, time factor and is define as

$$T = \left(\frac{\pi^2 k_1}{m_1\gamma_w l^2}\right) t \quad (2.41)$$

and

$$C_{v1} = \frac{k_1}{m_1\gamma_w} \quad (2.42)$$

Where C_{v1} = Consolidation coefficient for layer 1, m_1 = compressibility coefficient for layer 1 and γ_w = unit weight of water. Therefore, time factor T_v is given as:

$$T_v = \left(\frac{\pi^2 c_1}{H^2}\right) t \quad (2.43)$$

2.3.1 Degree of consolidation, *U*

The degree of consolidation *U* attained by a given soil layer at any given time is the ratio of consolidation settlement at any time to maximum consolidation settlement. It depends on its time factor, T_v. The time factor itself depends on the clay layer thickness H, number of drainage faces, coefficient of permeability k, and coefficient of compressibility m_v and the magnitude of the consolidation pressure distributed across the layer thickness. The mathematical expression of degree of consolidation *U*, is given by an infinite series: (Singh, 2002)

$$U = 1 - \frac{8}{\pi^2}\left[e^{-\frac{\pi^2}{4}T_v} + \frac{1}{9}e^{-\frac{9\pi^2}{4}T_v} + \frac{1}{25}e^{-\frac{25\pi^2}{4}T_v} + \cdots\right] \quad (2.44)$$

Where $T_v = \frac{\pi}{4}\left(\frac{U}{100}\right)^2$ when $U < 60\%$ and

$T_v = -0.9332\log_{10}\left(1 - \frac{U}{100}\right) - 0.0851$ when $U > 60\%$

The values of *Tv* corresponding to different degree of consolidation under different drainage and loading condition is given in Table 2.2 (Singh, 2002).

Table 2.2: Value of T_v Corresponding with value of U

Boundary conditions U (%)	T_v
5	0.002
10	0.008
15	0.018
20	0.031
25	0.049
30	0.071
35	0.096
40	0.126
45	0.159
50	0.197
55	0.238
60	0.287
65	0.342
70	0.403
75	0.477
80	0.567
85	0.684
90	0.848
95	1.129
100	∞

(Source: Singh, 2002)

In practice, the degree of consolidation value at 50%, U_{50} and 100%, U_{100} can be determine from the curve of deformation vs time obtained from laboratory tests result

using any of the two curve-fittings method suggested by Casagrande and Taylor (Singh, 2002).

2.3.2 Coefficient of consolidation C_v

The term, coefficient of consolidation c_v as used in the consolidation equations indicates the combined effects of permeability k, and compressibility m_v of a soil on the rate of volume change. As the void ratio of a soil decrease, both k and m_v decrease rapidly. However, c_v which depends on the ratio k/m_v remains constant. The unit of c_v are cm^2/sec, k in cm/sec while mv in cm^2/g and γ_w in g/cm^3 (Singh, 2002)

There are several procedures available for the estimation of coefficient of consolidation c_v, some of which are Casagrande's and Taylor's curve-fittings method, Su's maximum slope method, computational method, and Empirical correlation method, among others. The two common laboratory methods that is used for the determination of coefficient consolidation coefficient c_v are Casagrande logarithm of Time Fitting Method and Taylor Square Root of Time Fitting Method (Murthy, 2007). The scope of this work shall be limited to square root of time method as described by Taylor.

2.3.3 Taylor's square root of time method, $\sqrt{t}$

According to Arnold (2004), to determine the value of the coefficient of consolidation is to use only the results of a consolidation test for small values of time, and to use the fact that in the beginning of the process its progress is proportional to the square root of time. The consolidation measurement data are plotted against square root of time, $\sqrt{t}$, as shown in Figure 2.4. The basic equation is given.

$$\Delta h - \Delta h_0 = (\Delta h_\infty - \Delta h_0)\frac{2}{\sqrt{\pi}}\sqrt{\frac{c_v t}{h^2}} \tag{2.47}$$

In principle the value of the coefficient of consolidation c_v could be determined from the slope of the straight line in the figure, but this again requires the value of the initial

deformation and the final deformation, as these appear in the Eq. 2.25. The value of the initial deformation h_0 can be determined from the intersection point of the straight tangent to the curve with the axis $\sqrt{t} = 0$. The final deformation Δh_∞ cannot be obtained directly from the data. In order to overcome this difficulty Taylor has suggested to use the result following from the theoretical curve and its approximation that for U = 90% of the consolidation, the value of $\sqrt{t}$ according to the exact solution is 15% larger that the value given by the approximate Eq. 2.25. The approximate equation is given that U = 90% if $\frac{c_v t}{h^2} = 0.8481$, and U = 90% if $\frac{c_v t}{h^2} = 0.6362$. The ratio of these two values is 1.333, which is the square of 1.154.

This means that if in Figure 2.4 a straight line is plotted at a slope that is 15 percent smaller than the tangent to the measurement data for small values of time, this line should intersect the measured curve in the point for which U = 90%. The corresponding value of the time parameter $\frac{c_v}{h^2}$ is 0.848, and therefore the consolidation coefficient equation is given by;

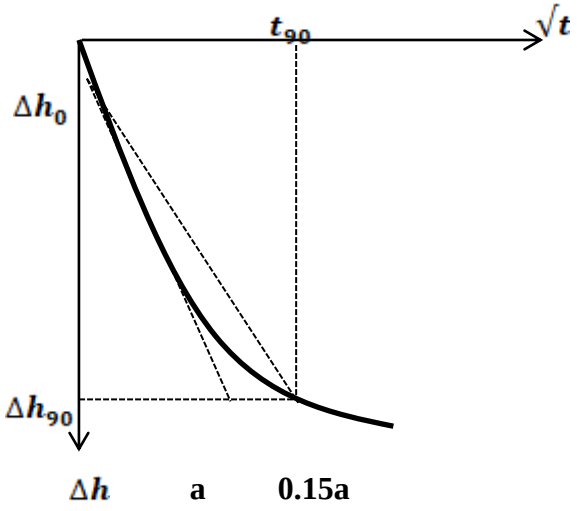

Figure 2.4: Square root of time curve

CHAPTER THREE

3.0 MATERIALS AND METHODS

3.1 Preamble

This chapter covers material, test and the method adopted in this study.

3.2 Materials

The materials used is mainly pan, water, spatula, 40mm height fabricated consolidation mould and ring and clayey soils collected from two different trial pits at different locations, namely College of Education Minna and Lapai Gwari, Niger State,

3.3 Method

The required soil samples are collected from different sampling locations using standard of specification for transportation material sampling and testing (AASHTO 2021). Samples collected from each location are properly labelled inside polyethylene and transferred immediately to the laboratory for test and analysis. The two different types of clay soil samples collected from different locations were combined to form a double layered soil element. Index properties and oedometer consolidation test were carried out on each soil sample and the results determined are used to validate the analytical model under review. The corresponding values of coefficient of consolidation c_v for each load increment are analysed from the relationship $cv = Tvd2/t_{90}$ were $Tv = 0.848$ for U_{90} and tabulated in Table 4.4 and 4.7 respectively.

3.3.1 Index properties of clay soil

The following properties were determined in the laboratory as described below.

(i) Liquid limit

(ii) Moisture content

(iii) Plastic limit

(iv) Specific gravity

(v) Particles size distribution – sieve analysis

(vi) Oedometer consolidation test

3.3.1.1 *Grain size analysis (Mechanical sieve analysis)*

This test covers the quantities determination of the particles size distribution in the soil mass down to the fine grain size. This test was performed in accordance with BS 1377 (1990). Section 2.7. The soil sample were dried properly and weighed to a total mass of 500g. The BS test sieves are cleaned, carefully weighed using the weighing balance and the weight were recorded. The samples were finely grinded with mortar and pestle without destroying the physical properties of the soil samples. The test sieves were properly arranged over each other, the measured soil sample will be poured into the set of sieves and placed on the electric sieve shaker and clamped, the arrangement which will then be subjected to vibration for 10 minutes for separation into various constituent according to sieve sizes.

The amount of soil sample retained in each sieve and the pan were weighed and recorded, then a graph of cumulative percentage passing against particle size was plotted.

Mass passing = individual mass retained - total mass retained.

Cumulative percentage passing = $\frac{mass\ passing}{total\ mass}$ x 100 (3.1)

3.3.1.2 *Natural moisture content*

The moisture content is a measure of the total water present in a soil sample.

Moisture cans were labelled and weighed as M_1 and collected soil samples will then be poured into the can and weighed as M_2. The cans containing the wet soil samples were

oven dry at 105ºC to dry to constant weight for complete 24 hours. The dried soil and cans will be removed after 24 hours and weighted as M_3; the natural moisture content (w) was calculated as:

$$w = \frac{(M_2 - M_3)}{(M_3 - M_1)} x\ 100 \qquad (3.2)$$

w = Natural moisture content

M_1 = Weight of empty moisture can.

M_2 = weight of moisture can + wet sample.

M_3 = weight of moisture can plus dried sample.

3.3.1.3 *Liquid limit*

Liquid Limit of a soil is the moisture content at which a mixture of a fraction of soil passing the 425ῡm BS sieve changes from a state of viscous limit to plastic limit.

200g of air-dried soil sample passing through 425ῡm specific gravity sieve were thoroughly mixed with distilled water to form uniform paste using the palette knives. The paste with the aid of the palette knives were placed into a small cylindrical metallic container and placed under the cone penetrometer to measure liquid limits as the water content in the soil sample. The standard cone penetrometer penetrates the soil 20mm for about five (5) seconds. Two readings were taken from each trial, that is, the first penetration for the first trial is repeated after filling the penetrated mark with the paste from that mix.

The average of the first and second reading of each trial was taken with water added to each of the successful trial and their readings taken. Several of trials will be made and their readings taken.

3.3.1.4 *Plastic limit*

Plastic limit of a soil is the water content at which a soil begins to crumble when rolled into a tinning thread approximately 3mm in diameter.

About 50g of soil sample passing through 425῀μm BS sieve were thoroughly mixed on a glass plate with enough water to make it homogenously and plastic enough to roll into ball. The ball paste was moulded between the palms of the hand until it formed a thread. The thread was rolled between the tips of the fingers of one hand until a thin thread of 3mm diameter was formed.

The above step was repeated until a 3mm diameter thread show signs of crumbling. Some grains of interest of the thread that is about crumbling were taken into container to give the average plastic limit and put inside oven to oven dry for 24hours.

The weight of each container and the weight of the container plus the samples were weighed before and after drying.

3.3.1.5 *Specific gravity*

The specific gravity of a soil is the weight of a given volume of soil particle to the weight of an equal volume of water.

A mass of the volumetric bottle was weighed and taken as M_1. 200g of soil sample were carefully poured into the volumetric bottle and weighed as M_2. About 300-500ml of water were added to the soil sample. The volumetric bottle was shaken thoroughly with rubber cork covered for 10minutes to remove any air and suspended particles in the sample and allowed to settle properly and reweighed as M_3.

Volumetric bottle filled with water to the brim and covered with the glass plate carefully in order not to trap any air under the plate. The water outside the bottle were cleaned carefully and weighted as M_4.

Specific gravity $Gs = \frac{(M_2 - M_1)}{(M_4 - M_1) - (M_3 - M_2)}$ (3.3)

Where

M_1 = Mass of empty bottle

M_2 = Mass of empty bottle + clay soil

M_3 = Mass of bottle + soil + water

M_4 = Mass of bottle + water only

3.3.2 *Oedometer consolidation test*

Oedometer consolidation test were carried out to determination the consolidation properties of single and double layered saturated clayey soil.

An empty consolidation ring together with the glass plate was weigh. The height, h and inside diameter of the ring will be measured and recorded.

A representative soil sample for the test were extruded and cut carefully from the soil block and ensured that the two plane faces of the disc of soil are parallel to each other, whose thickness is greater than the height of the consolidation ring.

Approximately three-inch-long of the sample will be cut and place in the consolidation ring. The top and bottom surface, above and below the edges of the ring were trimmed off, using the thin-bladed trimming knife and straightedge, until they are level and flush with the top and bottom edges of the ring.

During the trimming process, the sample were pressed into the ring gently to protrude a short distance through the bottom of the ring. Care were taken to avoid voids space between the sample and the ring. A glass plate previously weigh was placed on the freshly cut surface and the ring were turned to trim the bottom surface. Specimen plus ring plus glass plate were weighed.

The porous stones were centred on top and bottom surfaces of the test specimen. Filter papers were placed between porous stone and soil specimen. The assembly were lowered carefully into the base of water reservoir filled with water until the specimen is completely saturated.

The consolidation cell was placed in position on the bed of the loading apparatus and the counterbalance loading beam were adjusted into a level position with the appropriate load transmitting member in contact with the load cap.

The dial gauge was clamped into position and adjusted to a zero reading for recording the relative movement between the base of the consolidation cell and the loading cap.

An initial load of 25 kN/m^2 was hanged on the hanger to apply pressure on the specimen at a convenient moment as indicated by the stopwatch set properly to obtain accurate reading.

The reading of the compression gauge was taken at suitable interval of time for easy plotting at interval of 0, 0.125, 0.25, 0.5, 1, 2, 4, 8, 15,30,60 min and 2, 4, 8, 16, and 24 hours after the application of the pressure. The loading was repeated for 25, 50, 100, 200, 400, 800, 1600 and 3200 kN/m^2 respectively after every 24 hours of the day and the respective time reading were also taken.

After taken the last gauge reading under the maximum applied pressure, the load was removed from the test specimen gradually at a regular interval of time and the final dial reading and time were recorded. The consolidation cell was removed from the apparatus; the soil specimen and ring were placed on glass plate and weigh together.

Empty large moisture can, and lid were weighed to receive soil sample. The wet sample removed from the consolidation ring was placed in the empty moisture can. The sample plus the can were oven dried for 12 hours. The dried specimens in the moisture can were weighed to determine the final moisture content.

The relationships are given in equation 3.4 – 3.6

$$H_s = \frac{m_s \text{ x } 1000}{G_s \text{ x } \rho_w \text{ x A}} \tag{3.4}$$

Where.

H_s = height of the solid particle

G_s = specific gravity of the soil particles

m_s = the dry mass of specimen (g)

A = the area of the specimen (mm^2)

ρ_w = the dry density of water (mg/m^3)

$$e_0 = \frac{H_i - H_s}{H_s} \tag{3.5}$$

And

$$e_f = \frac{H_f - H_s}{H_s} \text{ or} \tag{3.6a}$$

$$e_f = mc_f \text{ x } G_s \quad (3.6b)$$

Where

e_0 = the void ratio before test

H_i = Initial height before test (mm)

mc_f = Final moisture content

G_s = specific gravity

$$m_v = \frac{dH}{H} \text{ x } 10 \quad (3.7a)$$

Or

$$m_v = \frac{de}{1+e_0} \text{ x } 10 \quad (3.7b)$$

Where

m_v = coefficient of volume compressibility

dH = change in thickness

H = the thickness of specimen under effective pressure

de = the change in voids ratio corresponding to the increment of 100 kN/m^2

e = the voids ratio under the present effective pressure.

3.3.2.1 *Consolidation of double layered clay soil*

To illustrate the consolidation theory of the multiple layered soil, a thin layer, $h_{1\text{-}2}$ = 20mm in thickness of sample 1, and sample 2 were extracted from their individual undisturbed sample block and combined together to form a multiple layered clay of thickness H = 40mm.

The multiple layered clay elements with their individual consolidation properties were determined separately. The consolidation procedure carried out on each of the clay sample were repeated for the combined clay sample so as to show the behaviours of the multiple layered clay sample under an applied effective pressure with time and double drainage condition.

3.4 Model Validation

3.4.1 Distribution of excess pore water pressure

The analytical model under review was validated in terms of distribution of excess pore water pressure with 7 days experimental data of consolidation test conducted on two different soil sample obtained at a different location. The index properties of the soils sample under study were determined and curve fitted parameters were used as modelling parameters, having obtained from deformation plots against square root of time based on Eq. 2.43.

However, the analytical model shows the consolidation behaviours of double – layered clayey soil in terms of excess pore water pressure profile at any given time t and depth z, under double drainage conditions. Eq. 29 and 46 (Sadiku, 1991).

To demonstrate the application of this analytical model, the excess pore water pressure for the combined soil element is determined based on Eq. 3.8, 3.9 and 3.10 and

compared with other scholar's works. The two layers are equal in thickness, each of h_1 = h_2 = 20 mm (H = 40 mm). The consolidation parameters of the first and second layer which were determined through oedometer test after seven days of consolidation test were tabulated. The initial excess pore water pressure is taken to be u_0 =100 kN/m2 distributed uniformly throughout the soil layer. The soil sample was allowed to drain both top and bottom. To calculate the distribution of excess pore water pressure based on the proposed model, Eq. 3.8 was considered for single layer soil.

However, the distribution of excess pore pressure u for double layered clay soil in terms of time t and depth z was determine from Eq. 3.10, 3.11 and 3.12

$u(z,t) = \sum_{j=1}^{3} e^{-\omega_j T} \phi_j(z)$ (Sadiku 1991)

$$u(z,t) = \left\{ e^{-0.0687T} v \left(0.8255 \sin\frac{\pi z}{l} - 0.3418 \sin\frac{2\pi z}{l} - 0.0471 \sin\frac{3\pi z}{l} \right) + e^{-0.2816T} v \left(0.2606 \sin\frac{\pi z}{l} + 0.6986 \sin\frac{2\pi z}{l} - 0.5491 \sin\frac{3\pi z}{l} \right) + e^{-1.6660T} v \left(0.2944 \sin\frac{\pi z}{l} + 0.5701 \sin\frac{2\pi z}{l} + 0.8155 \sin\frac{3\pi z}{l} \right) \right\}$$

$v = (m_1 \gamma_w l)^{-1/2}$ And $T = \left(\frac{\pi^2 c v_1}{l^2}\right) t$

$v = (3.053 \text{ x } 10^{-4} \text{x } 9.81 \text{ x } 0.02)^{-1/2}$

$v = 129.21$

$T = \left(\frac{\pi^2 \text{ x } 5.466 \text{ x } 10^{-6}}{0.02^2}\right) t$ = 0.1349t

Therefore,

$$u(z,t) = \left\{e^{-0.009267844t}\left(106.66\ sin\frac{\pi z}{l} - 44.16\ sin\frac{2\pi z}{l} - 6.09\ sin\frac{3\pi z}{l}\right) + e^{-0.03933775t}\left(33.67\ sin\frac{\pi z}{l} + 90.26\ sin\frac{2\pi z}{l} - 70.95\ sin\frac{3\pi z}{l}\right) + e^{-0.2247486t}\left(38.04\ sin\frac{\pi z}{l} + 73.66\ sin\frac{2\pi z}{l} + 105.37\ sin\frac{3\pi z}{l}\right)\right\} \quad (3.8)$$

At the first layer

$u(z,t) = \sum_{j=1}^{3} e^{-\omega_j T}\phi_j(z)$ (Sadiku 1991)

$$u(z,t) = \left\{e^{-0.0687T}v\left(0.8255\ sin\frac{\pi z}{l} - 0.3418\ sin\frac{2\pi z}{l} - 0.0471\ sin\frac{3\pi z}{l}\right) + e^{-0.2816T}v\left(0.2606\ sin\frac{\pi z}{l} + 0.6986\ sin\frac{2\pi z}{l} - 0.5491\ sin\frac{3\pi z}{l}\right) + e^{-1.6660T}v\left(0.2944\ sin\frac{\pi z}{l} + 0.5701\ sin\frac{2\pi z}{l} + 0.8155\ sin\frac{3\pi z}{l}\right)\right\}$$

$v = (m_1\gamma_w l)^{-1/2}$ And $T = \left(\frac{\pi^2 c v_1}{l^2}\right)t$

$v = (3.053 \text{ x } 10^{-4} \text{x } 9.81 \text{ x } 0.04)^{-1/2}$

$v = 91.3634$

$T = \left(\frac{\pi^2 \text{ x } 5.466 \text{ x } 10^{-6}}{0.04^2}\right)t = 0.03373t$

Therefore,

$$u_1(z,t) = \left\{e^{-0.00231696t}\left(75.4205\ sin\frac{\pi z}{l} - 31.2280\ sin\frac{2\pi z}{l} - 4.3032\ sin\frac{3\pi z}{l}\right) + e^{-0.0098344t}\left(23.8093\ sin\frac{\pi z}{l} + 63.8265\ sin\frac{2\pi z}{l} - 50.1676\ sin\frac{3\pi z}{l}\right) + e^{-0.0561872t}\left(26.897\ sin\frac{\pi z}{l} + 52.0863\ sin\frac{2\pi z}{l} + 74.5068\ sin\frac{3\pi z}{l}\right)\right\} \quad (3.9)$$

At the common boundary, excess pore water pressure is given by Eq. (2.40)

$$u(z,t) = \left\{ e^{-0.00231696t}\Omega_1 \left(75.421 sin\frac{\pi z}{l} - 31.228\ sin\frac{2\pi z}{l} - 4.303\ sin\frac{3\pi z}{l}\right) + \right.$$
$$e^{-0.00983444t}\Omega_2 \left(23.8093\ sin\frac{\pi z}{l} + 63.8265\ sin\frac{2\pi z}{l} - 50.1676\ sin\frac{3\pi z}{l}\right) +$$
$$\left. e^{-0.05618715t}\Omega_3 \left(26.897 sin\frac{\pi z}{l} + 52.086 sin\frac{2\pi z}{l} + 74.507 sin\frac{3\pi z}{l}\right)\right\} \quad (3.10)$$

Given that

$$\Omega_{rr} = -\frac{k_1\pi}{2l}\left\{r^2\pi\left[\alpha + (1-\alpha)\left(\lambda + \frac{\sin 2r\lambda\pi}{2\,r\pi}\right)\right] - \psi_j\pi\left[\beta + (1-\beta)\left(\lambda - \frac{\sin 2r\lambda\pi}{2r\pi}\right)\right]\right\}$$

Where $\psi_j = \left(\frac{m_1\gamma_w l^2}{k_1\pi^2}\right)\omega_j$,

$$\psi_1 = \left(\frac{3.053\ x\ 10^{-4}\ x\ 9.81\ x\ 0.04^2}{1.64\ x\ 10^{-8}\pi^2}\right) 0.0687 = 2.0334$$

$$\psi_2 = \left(\frac{3.053\ x\ 10^{-4}\ x\ 9.81\ x\ 0.04^2}{1.64\ x\ 10^{-8}\pi^2}\right) 0.2816 = 8.3347$$

$$\psi_3 = \left(\frac{3.053\ x\ 10^{-4}\ x\ 9.81\ x\ 0.04^2}{1.64\ x\ 10^{-8}\pi^2}\right) 1.6660 = 49.3100$$

$$\propto = \frac{k_2}{k_1} = \frac{1.11\ x\ 10^{-8}}{1.64\ x\ 10^{-8}} = 6.7683\ x\ 10^{-17}$$

$$\beta = \frac{m_2}{m_1} = \frac{1.659\ x\ 10^{-4}}{3.053\ x\ 10^{-4}} = 5.4340\ x\ 10^{-9}$$

$$\lambda = \frac{h_2}{h_1} = \frac{0.02}{0.02} = 1$$

Ω_1

$$= -\frac{k_1\pi}{2l}\left\{\pi\left[6.7683\ x\ 10^{-17} + (1 - 6.7683\ x\ 10^{-17})\left(1 + \frac{\sin 2\pi}{2\,\pi}\right)\right] - \right.$$
$$\left. 2.0334\pi\left[5.4340\ x\ 10^{-9} + (1 - 5.4340\ x\ 10^{-9})\left(1 - \frac{\sin 2\pi}{2\pi}\right)\right]\right\}$$

Ω_1

$$= -\frac{k_1\pi}{2l}\{\pi[6.7683\ x\ 10^{-17} + (1)(1.0174)] - 2.0334\pi[5.4340\ x\ 10^{-9} + (1)(0.9826)]\}$$

$$\Omega_1 = -6.4411\ x\ 10^{-7}\{3.1967 - 6.2778\}$$

$$\Omega_1 = 1.98457\ x\ 10^{-6}$$

Ω_2

$$= -\frac{k_1\pi}{2l}\left\{4\pi\left[6.7683\ \text{x}\ 10^{-17} + (1 - 6.7683\ \text{x}\ 10^{-17})\left(1 + \frac{\sin 2\text{x}2\pi}{2\ \text{x}\ 2\pi}\right)\right] - 8.3347\pi\left[5.4340\ \text{x}\ 10^{-9} + (1 - 5.4340\ \text{x}\ 10^{-9})\left(1 - \frac{\sin 2\text{x}2\pi}{2\text{x}2\pi}\right)\right]\right\}$$

Ω_2

$$= -\frac{k_1\pi}{2l}\{4\pi[6.7683\ \text{x}\ 10^{-17} + 1(1.0173)] - 8.3347\pi[5.4340\ \text{x}\ 10^{-9} + 1(0.9827)]\}$$

$$\Omega_2 = -6.4411\ \text{x}\ 10^{-7}\{12.7854 - 25.7345\}$$

$$\Omega_2 = 8.34068\ \text{x}\ 10^{-6}$$

Ω_3

$$= -\frac{k_1\pi}{2l}\left\{9\pi\left[6.7683\ \text{x}\ 10^{-17} + (1 - 6.7683\ \text{x}\ 10^{-17})\left(1 + \frac{\sin 2\text{x}3\pi}{2\ \text{x}\ 3\pi}\right)\right] - 49.310\pi\left[5.4340\ \text{x}\ 10^{-9} + (1 - 5.4340\ \text{x}\ 10^{-9})\left(1 - \frac{\sin 2\text{x}3\pi}{2\text{x}3\pi}\right)\right]\right\}$$

Ω_3

$$= -\frac{k_1\pi}{2l}\{9\pi[6.7683\ \text{x}\ 10^{-17} + 1(1.0173)] - 49.31\pi[5.4340\ \text{x}\ 10^{-9} + 1(0.9827)]\}$$

$$\Omega_3 = -6.4411\ \text{x}\ 10^{-7}\{28.7672 - 152.2516\}$$

$$\Omega_3 = 7.95375\text{x}\ 10^{-5}$$

Therefore,

$$u(z,t) = \left\{e^{-0.002317t}\left(0.000150\ sin\frac{\pi z}{l} + 0.000062\ sin\frac{2\pi z}{l} + 0.00000854\ sin\frac{3\pi z}{l}\right) + e^{-0.009834t}\left(0.0001986\ sin\frac{\pi z}{l} - 0.00053236\ sin\frac{2\pi z}{l} + 0.00041844 sin\frac{3\pi z}{l}\right) + e^{-0.0562t}\left(0.0021394 sin\frac{\pi z}{l} + 0.0041428 sin\frac{2\pi z}{l} + 0.0059261 sin\frac{3\pi z}{l}\right)\right\} \quad (3.11)$$

At the Second Layer

$$u_2(z,t) = \left\{e^{-0.0687T} v\left(0.8255\ sin\frac{\pi z}{l} - 0.3418\ sin\frac{2\pi z}{l} - 0.0471\ sin\frac{3\pi z}{l}\right) + e^{-0.2816T} v\left(0.2606\ sin\frac{\pi z}{l} + 0.6986\ sin\frac{2\pi z}{l} - 0.5491\ sin\frac{3\pi z}{l}\right) + e^{-1.6660T} v\left(0.2944\ sin\frac{\pi z}{l} + 0.5701\ sin\frac{2\pi z}{l} + 0.8155\ sin\frac{3\pi z}{l}\right)\right\}$$

$v = (m_2 \gamma_w l)^{-1/2}$ And $T = \left(\frac{\pi^2 c v_2}{l^2}\right) t$

$v = (1.659 \text{ x } 10^{-4} \text{x } 9.81 \text{ x } 0.04)^{-1/2}$

$v = 123.9402$

$T = \left(\frac{\pi^2 \text{ x } 6.808 \text{ x } 10^{-6}}{0.04^2}\right) t = 0.04201t$

Therefore,

$$u_2(z,t) = \left\{ e^{-0.002886t} \left(102.313 \sin\frac{\pi z}{l} - 42.363 \sin\frac{2\pi z}{l} - 5.838 \sin\frac{3\pi z}{l}\right) + e^{-0.01225t} \left(32.299 \sin\frac{\pi z}{l} + 86.585 \sin\frac{2\pi z}{l} - 68.056 \sin\frac{3\pi z}{l}\right) + e^{-0.06998t} \left(36.488 \sin\frac{\pi z}{l} + 70.658 \sin\frac{2\pi z}{l} + 101.073 \sin\frac{3\pi z}{l}\right) \right\} \quad (3.12)$$

The theoretical variation of excess pore water pressure u with depth z at a given time t, is obtained based on Eq. 3.10, 3.11 and 3.12.

CHAPTER FOUR

4.0 RESULTS AND DISCUSSION

4.1 Index Properties of Soil Samples

The index properties of the soils used in this study were presented in Table 4.1. The two soils samples are classified as clayey material belonging to group A-7-5(8) and A-7-5(20) in accordance with AASHTO system of soil classification (2021) and Braja (2019)

Table 4.1: Index Properties

	Sample Identification		
Test Name	Sample 1	Sample 2	Specification
Natural moisture content (%)	13	11	
Specific gravity	2.62	2.47	
Liquid limit (%)	41.09	41.66	41 (min)
Plastic limit (%)	18.97	28.28	
Plasticity Index (%)	22.12	13.38	11 (min)
Passing sieve No. 200 (%)	5.53	65.7	
AASHTO classification	A-7-5(8)	A-7-5(20)	Clay

4.2 Oedometer Consolidation Test Results

Oedometer test were carried out on the two soils sample and the result gives an idea of the amount of consolidation of the soils on site and the rate at which it occurs.

4.2.1 One-dimensional consolidation of sample 1

Table 4.2 and Figure 4.1 to 4.6 shows the time – compression data of Oedometer test carried out on sample 1 and the plot of deformation against square root of time for each pressure increment at 24 hours' interval in the sequence; 12.5, 25, 50, 100, 200, 400, 800 and 1600 kN

/m^2 respectively.

The value of t_{90} at 90% consolidation, U_{90} of each load increment were determined using Taylor's square root of time method as obtained from Figure 4.1 – 4.6

The corresponding values of coefficient of consolidation c_{v1} for each load increment are analysed from the relationship cv = Tvd2/t_{90} were Tv = 0.848 for U_{90} and tabulated in Table 4.4 and 4.7 respectively.

Table 4.2: Time – Compression Data of Sample 1

Loading		1	2	3	4	5	6	7	8	9
Load (kN/m^2)		12.5	25	50	100	200	400	800	1600	12.5
Elapse time, t (min)	Square root of time (min)	Deformations (mm)								
0	0	20.00	20.00	20.00	19.87	19.26	18.30	17.49	16.62	15.81
0.08	0.29	20.00	20.00	19.98	19.59	18.93	17.88	17.08	16.31	16.14
0.17	0.41	20.00	20.00	19.98	19.58	18.91	17.87	17.06	16.30	16.15
0.25	0.5	20.00	20.00	19.97	19.56	18.90	17.86	17.05	16.29	16.15
0.5	0.71	20.00	20.00	19.97	19.54	18.87	17.84	17.02	16.27	16.16
1	1	20.00	20.00	19.96	19.51	18.84	17.82	17.00	16.24	16.17
2	1.41	20.00	20.00	19.96	19.48	18.80	17.79	16.97	16.21	16.19
4	2	20.00	20.00	19.95	19.45	18.77	17.75	16.94	16.18	16.22
8	2.83	20.00	20.00	19.94	19.42	18.72	17.72	16.90	16.15	16.26
16	3.87	20.00	20.00	19.93	19.40	18.69	17.69	16.87	16.12	16.31
30	5.48	20.00	20.00	19.92	19.37	18.65	17.65	16.83	16.08	16.37
60	7.75	20.00	20.00	19.91	19.34	18.61	17.61	16.78	16.02	16.45
120	10.95	20.00	20.00	19.90	19.32	18.58	17.57	16.73	15.96	16.55
240	15.49	20.00	20.00	19.89	19.30	18.54	17.54	16.68	15.90	16.69
480	21.91	20.00	20.00	19.88	19.28	18.48	17.51	16.65	15.83	16.80
960	30.98	20.00	20.00	19.87	19.27	18.41	17.50	16.63	15.82	16.85
1440	37.94	20.00	20.00	19.87	19.26	18.30	17.49	16.62	15.81	16.88

Graph of deformation against the square root of time recorded during consolidation procedure at first loading of 50 kN/m^2 was plot as shown in Figure 4.1. Using Taylor's square root of time method, the square root of time at 90% consolidation was determined; at $\sqrt{t_{90}}$ = 5.0min

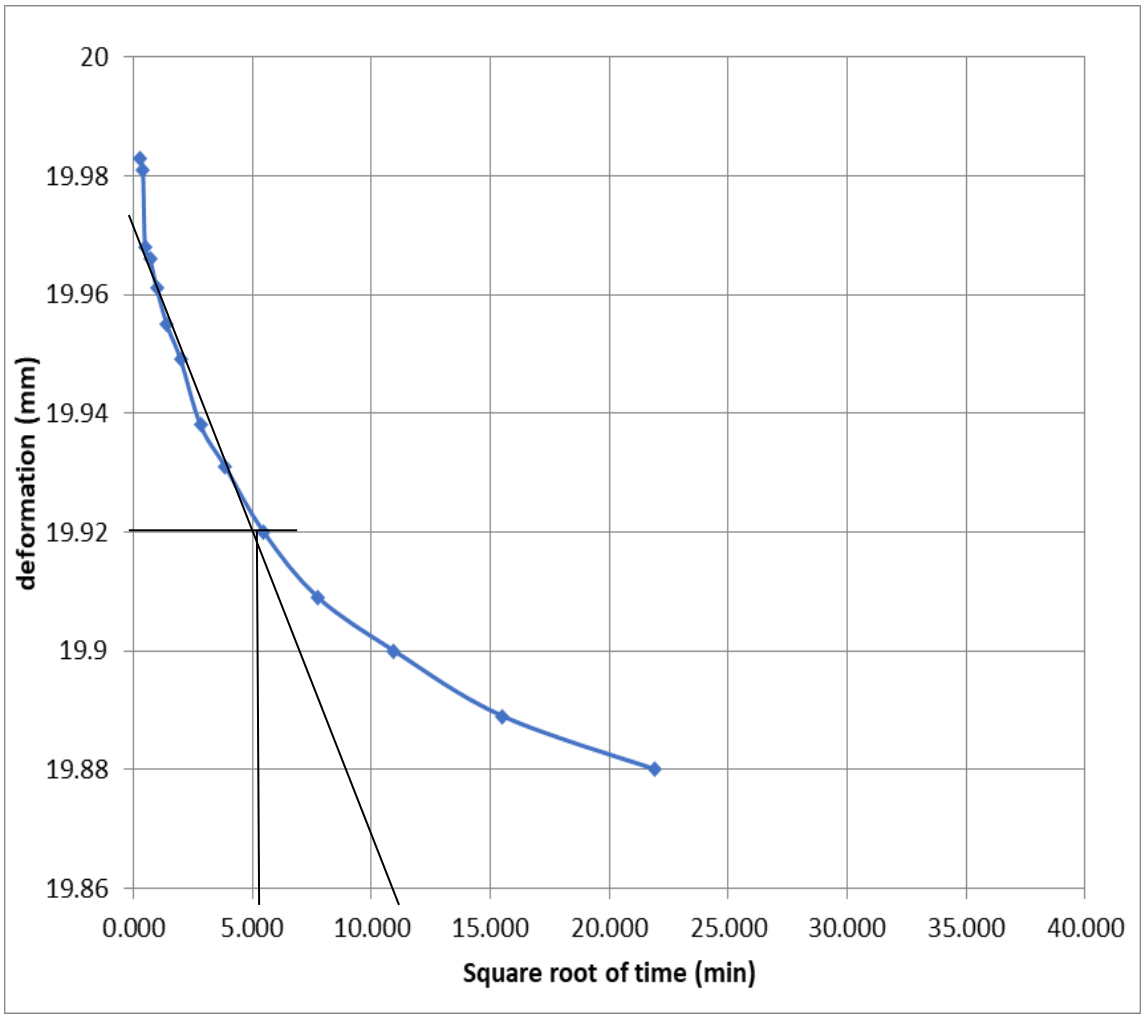

Figure 4.1: Deformation – Square root of time curve for 50 kN/m^2 ($\sqrt{t_{90}}$ = 5.0)

Graph of deformation against the square root of time recorded during consolidation procedure at first loading of 100 kN/m^2 was plot as shown in Figure 4.2. Using Taylor's square root of time method, the square root of time at 90% consolidation was determined; at $\sqrt{t_{90}}$ = 5.25min

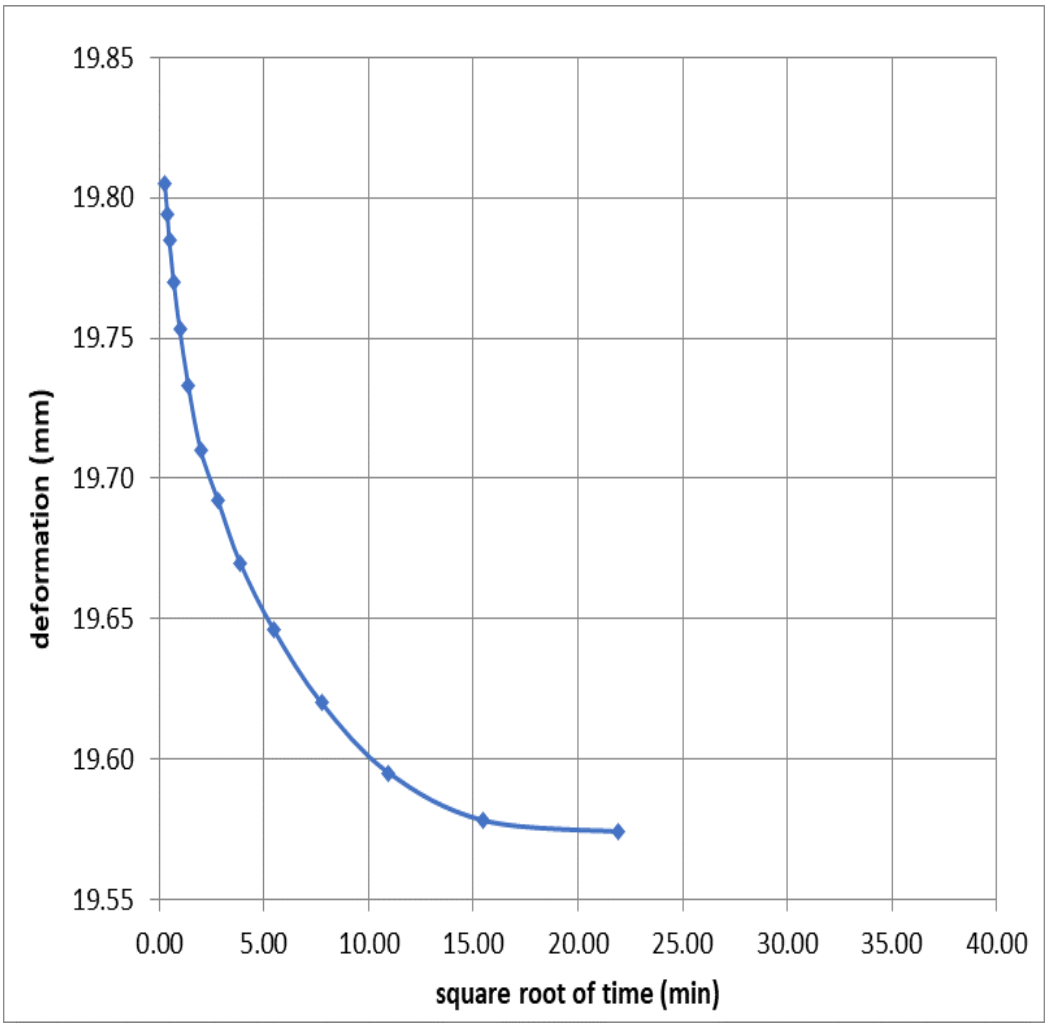

Figure 4.2: Deformation – Square root of time curve for 100 kN/m^2 ($\sqrt{t_{90}}$ = 5.25)

Graph of deformation against the square root of time recorded during consolidation procedure at first loading of 200 kN/m^2 was plot as shown in Figure 4.3. Using Taylor's square root of time method, the square root of time at 90% consolidation was determined; at $\sqrt{t_{90}}$ = 3.50min

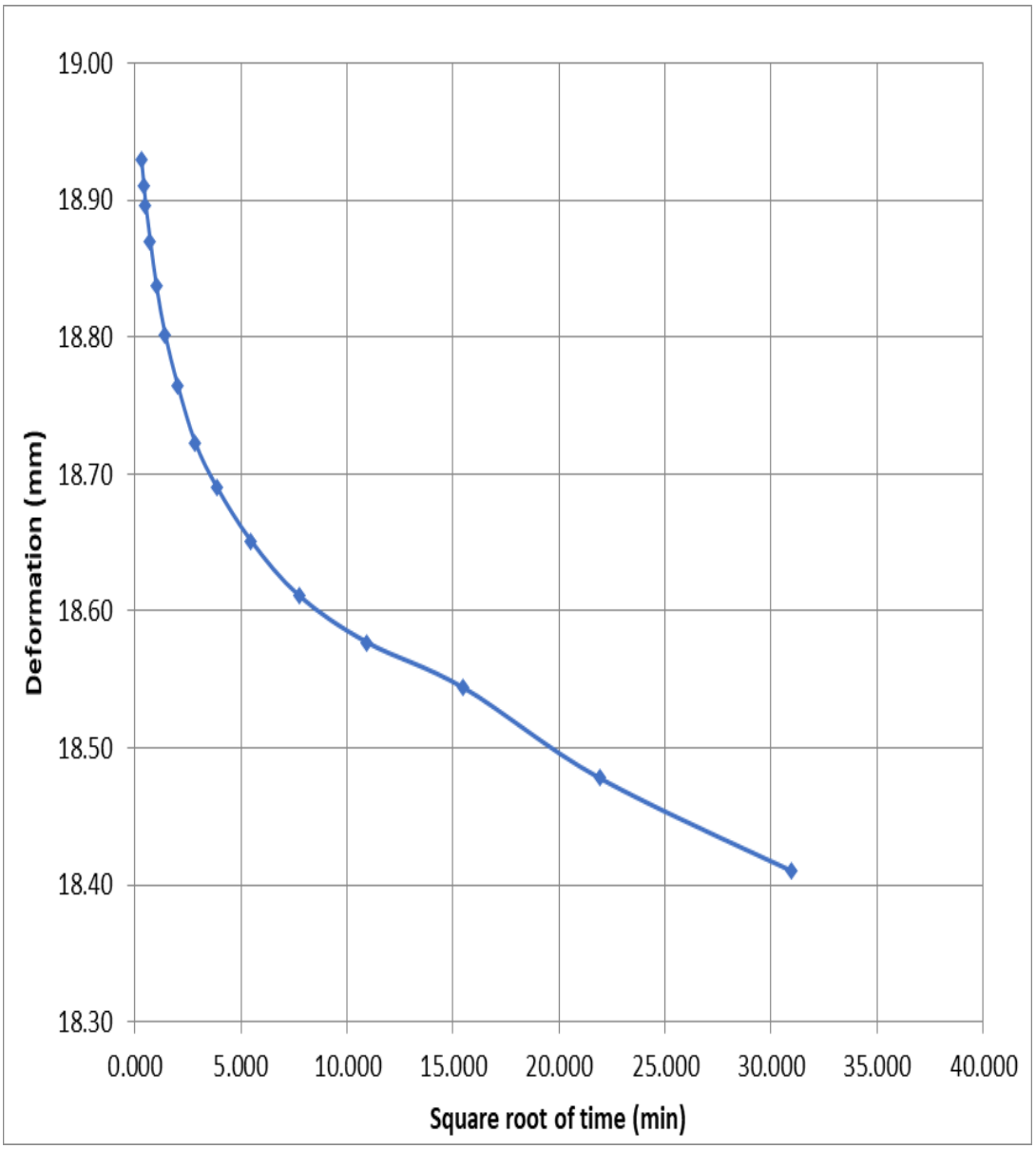

Figure 4.3: Deformation – Square root of time curve for 200 kN/m^2 ($\sqrt{t_{90}}$ = 3.50)

Graph of deformation against the square root of time recorded during consolidation procedure at first loading of 400 kN/m^2 was plot as shown in Figure 4.4. Using Taylor's square root of time method, the square root of time at 90% consolidation was determined; at $\sqrt{t_{90}}$ = 3.70min

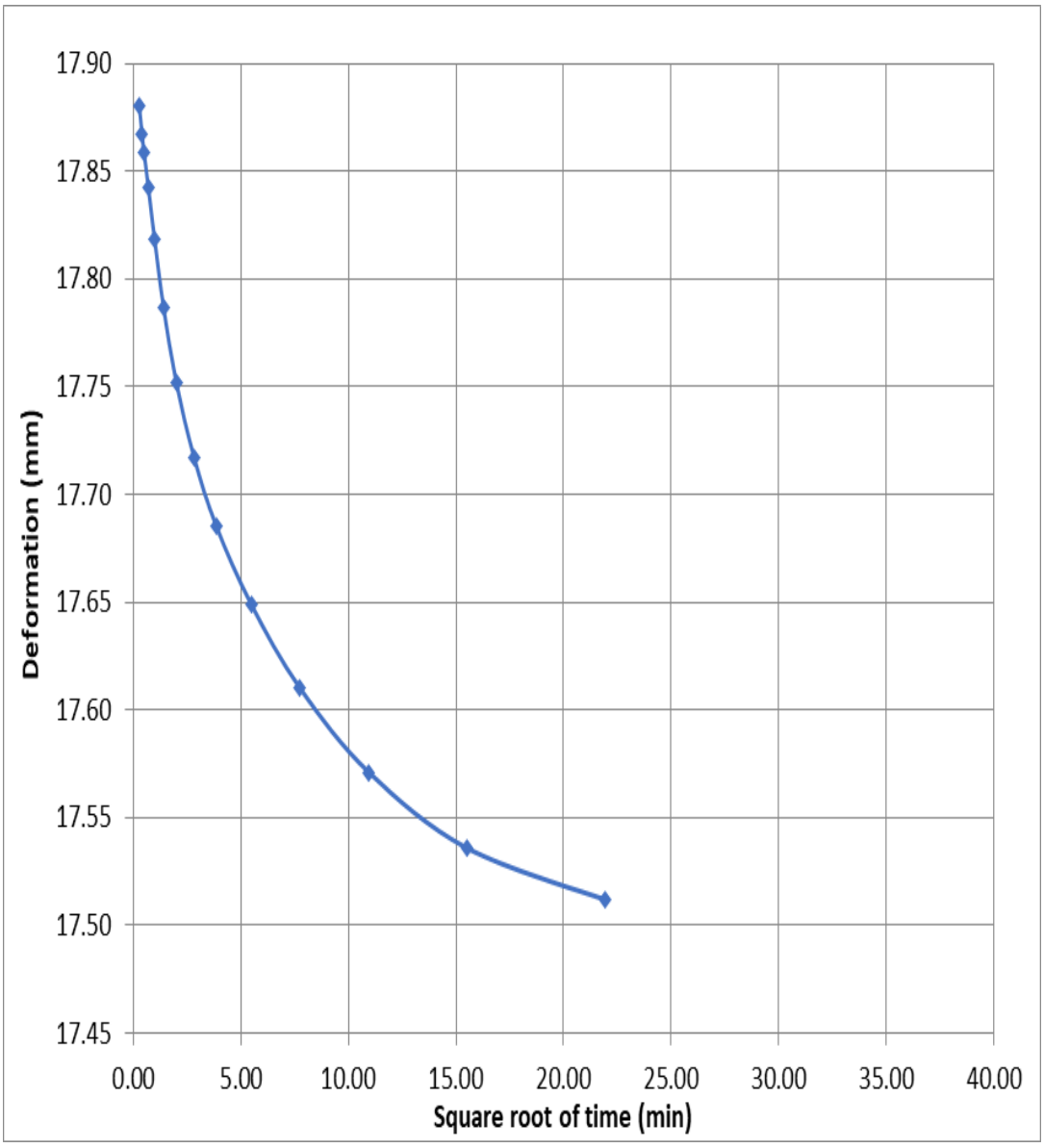

Figure 4.4: Deformation – Square root of time curve for 400 kN/m^2 ($\sqrt{t_{90}}$ = 3.70)

Graph of deformation against the square root of time recorded during consolidation procedure at first loading of 800 kN/m^2 was plot as shown in Figure 4.5. Using Taylor's square root of time method, the square root of time at 90% consolidation was determined; at $\sqrt{t_{90}}$ = 2.99min

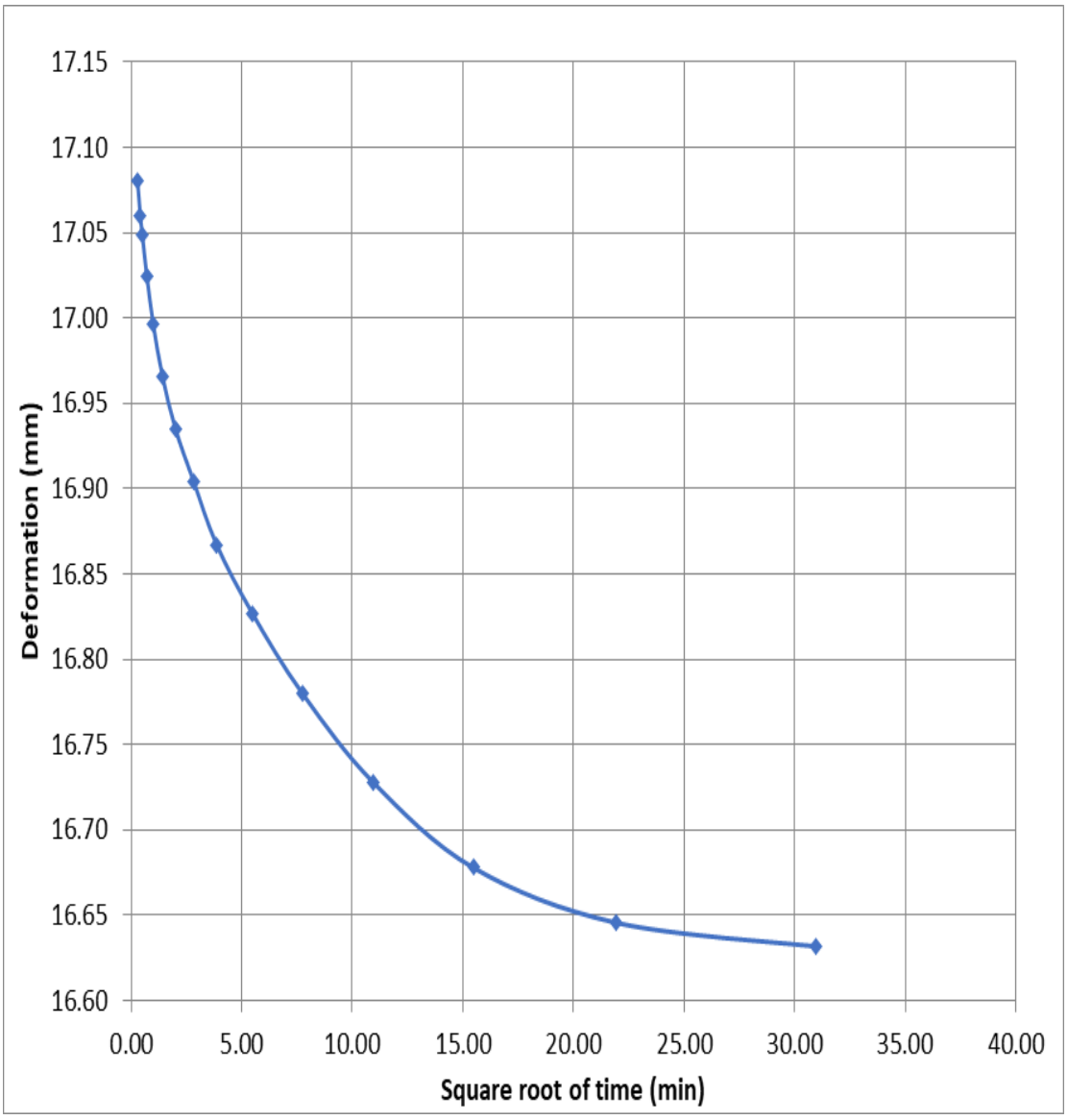

Figure 4.5: Deformation – Square root of time curve for 800 kN/m^2 ($\sqrt{t_{90}}$ = 2.99)

Graph of deformation against the square root of time recorded during consolidation procedure at first loading of 1600 kN/m^2 was plot as shown in Figure 4.6. Using Taylor's square root of time method, the square root of time at 90% consolidation was determined; at $\sqrt{t_{90}}$ = 3.80min

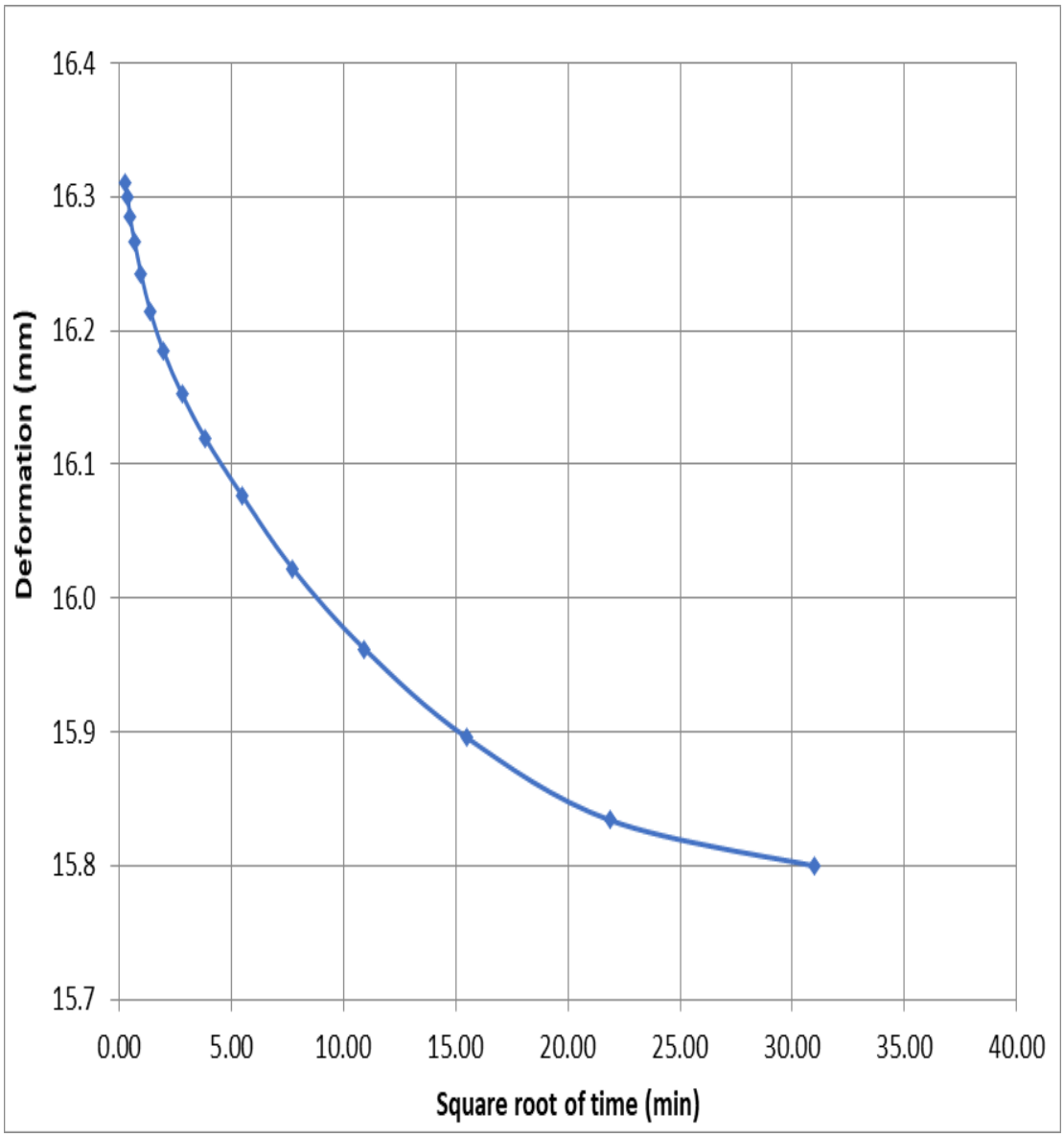

Figure 4.6: Deformation – Square root of time curve for 1600 kN/m^2 ($\sqrt{t_{90}}$ = 3.80)

The corresponding values of coefficient of consolidation c_{v1} for each load increment are analysed from the relationship $c_v = T_v d^2/t_{90}$ were $T_v = 0.848$ for U_{90} and results are presented in Table 4.3.

Table 4.3: Analysis of Consolidation Test Results – Sample 1

Applied pressure, σ (kN/m^2)	Time for 90% Consolidation t_{90} (min)	Specimen height H (m)	Sample Depth $d^2 = (H/2)^2$ (m)	$c_v = 0.848d^2/t_{90}$ (m^2/min)
50	25	0.0199	9.868E-05	3.347E-06
100	27.5625	0.0193	9.278E-05	2.854E-06
200	12.25	0.0183	8.369E-05	5.793E-06
400	13.69	0.0175	7.648E-05	4.737E-06
800	8.9401	0.0166	6.904E-05	6.549E-06
1600	14.44	0.0158	6.245E-05	3.667E-06

From Table 4.3, the coefficient of consolidation ranges from 2.8 x 10^{-6} m^2/min to 6.6 x 10^{-6} m^2/min depending on the applied pressure. The weighted average coefficient of consolidation within the applied pressure is calculated as follows:

$$C_{v1} = \frac{50}{1600} \text{x } 3.347 \text{ x } 10^{-6} + \frac{100}{1600} \text{x } 2.854 \text{ x } 10^{-6} + \frac{200}{1600} \text{x } 5.793 \text{ x } 10^{-6} + \frac{400}{1600} \text{x } 4.737 \text{ x } 10^{-6} + \frac{800}{1600} \text{x } 6.549 \text{ x } 10^{-6}$$

$$C_{v1} = 0.105 \text{ x } 10^{-6} + 0.178 \text{ x } 10^{-6} + 0.724 \text{ x } 10^{-6} + 1.184 \text{ x } 10^{-6} + 3.275 \text{ x } 10^{-6}$$

C_{v1} = 5.466 x $10^{-6}m^2$/min

4.2.1.1 *Void ratio of sample 1*

The final void ratio at the end of consolidation process is given by $e_f = mc_f$ x G_s

Given that, final moisture content,mc_f, of the soil sample is 18.82%, final height H_f is 16.88mm and specific gravity G_s is 2.62 as obtained from the laboratory test.

Therefore,

$$e_f = \frac{18.82}{100} \text{ x } 2.62$$

$$e_f = 0.493$$

$$\Delta e = \frac{1+e_f}{H_f} \text{ x } \Delta H$$

$$\Delta e = \frac{1+0.943}{16.88} \text{ x } \Delta H$$

$$\Delta e = 0.088\Delta H$$

The void ratios at each load increment are calculated and tabulated in Table 4.4. The graph of the relationship of void ratio – effective stress was plotted as shown in Figure 4.7

Table 4.4: Void Ratio Calculation – Sample1

Applied pressure (kN/m^2)	Change in thickness ΔH (mm)	Specimen height H (mm)	Change in voids ratio Δe = 0.088ΔH	Voids ratio e
12.5		20		
25		20		0.768
	-0.132		-0.012	
50		19.868		0.756
	-0.604		-0.053	
100		19.264		0.703
	-0.968		-0.085	
200		18.296		0.618
	-0.806		-0.071	
400		17.49		0.547
	-0.872		-0.077	
800		16.618		0.470
	-0.813		-0.072	
1600		15.805		0.398
	1.075		0.095	
12.5		16.88		0.493

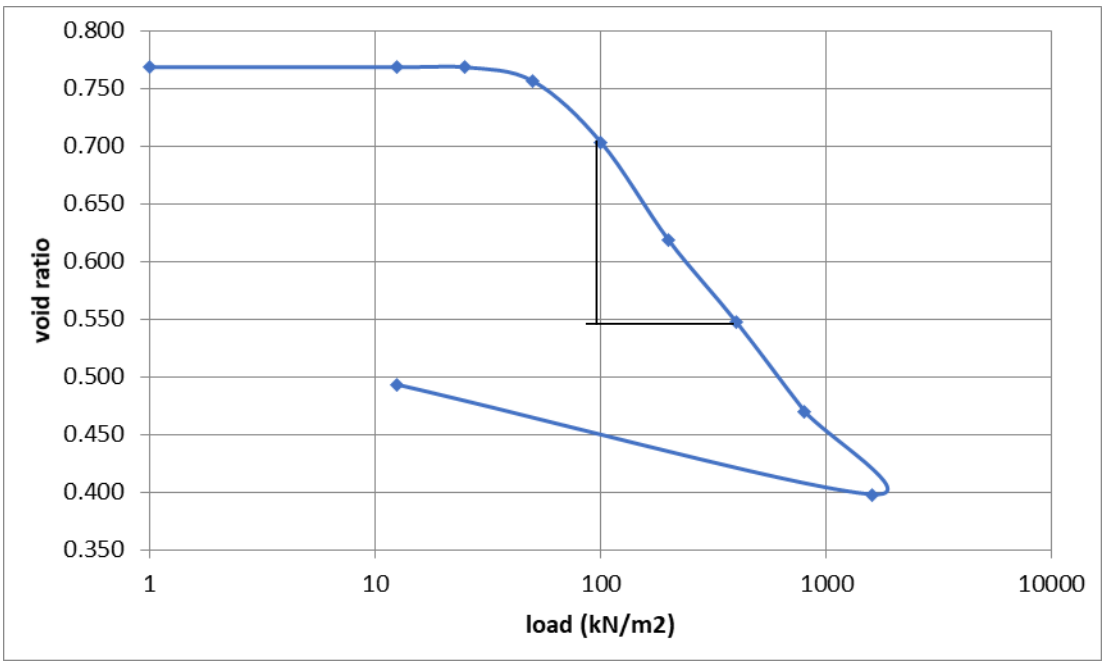

Figure 4.7: Void Ratio – Effective stress relationship

4.2.1.2 *Coefficient of compressibility of sample 1*

From Eq. 4.2, the coefficient of compressibility m_{v1} as follows

$$m_{v1} = -\frac{\Delta e}{1+e_0} \text{ x } \frac{1}{\Delta \sigma}$$

$$m_{v1} = -\frac{0.547-0.703}{1+0.703} \frac{1}{400-100} = \frac{0.156}{1.703} \text{ X } \frac{1}{300}$$

$$m_{v1} = 3.053 \text{ x } 10^{-4} \text{ m}^2/\text{kN}$$

4.2.1.3 *Coefficient of permeability of sample 1*

$$k_1 = c_{v1} \text{ x } m_{v1} \text{ x } \gamma_w$$

$$k_1 = 5.466 \text{ x } 10^{-6} \text{ x } 3.053 \text{ x } 10^{-4} \text{ x } 9.81$$

$$k_1 = 1.64 \text{ x } 10^{-8} \text{m/min}$$

4.2.2 One-dimensional consolidation of sample 2

Table 4.5 and Figure 4.8 to 4.13 shows the time – compression data of oedometer test carried out on soil sample 2 and the plot of deformation against square root of time for each pressure increment at 24 hours' interval in the sequence; 12.5, 25, 50, 100, 200, 400, 800 and 1600 kN/m^2 respectively.

Table 4.5: Time – Compression Data of Sample 2

Loading		1	2	3	4	5	6	7	8	9
Load (kN/m^2)		12.5	25	50	100	200	400	800	1600	12.5
Elapse time, t (min)	Square root of time (min)	Deformations (mm)								
0.08	0.29	20.00	20.00	19.99	19.81	19.41	18.98	18.49	18.01	17.35
0.17	0.41	20.00	20.00	19.99	19.79	19.40	18.96	18.48	18.00	17.26
0.25	0.5	20.00	20.00	19.99	19.79	19.39	18.96	18.47	17.99	17.36
0.5	0.71	20.00	20.00	19.99	19.77	19.37	18.94	18.46	17.98	17.38
1	1	20.00	20.00	19.99	19.75	19.35	18.92	18.44	17.95	17.39
2	1.41	20.00	20.00	19.98	19.73	19.33	18.89	18.42	17.92	17.40
4	2	20.00	20.00	19.98	19.71	19.31	18.85	18.39	17.87	17.41
8	2.83	20.00	20.00	19.98	19.69	19.28	18.81	18.35	17.80	17.42
16	3.87	20.00	20.00	19.97	19.67	19.25	18.76	18.30	17.72	17.43
30	5.48	20.00	20.00	19.97	19.65	19.21	18.73	18.23	17.58	17.43
60	7.75	20.00	20.00	19.96	19.62	19.17	18.70	18.13	17.42	17.43
120	10.95	20.00	20.00	19.95	19.60	19.15	18.69	18.12	17.25	17.44
240	15.49	20.00	20.00	19.95	19.58	19.13	18.65	18.11	17.19	17.44
480	21.91	20.00	20.00	19.94	19.57	19.11	18.63	18.09	17.16	17.45
960	30.98	20.00	20.00	19.94	19.56	19.08	18.63	18.08	17.13	17.45
1440	37.94	20.00	20.00	19.93	19.55	19.07	18.62	18.08	17.12	17.45

Graph of deformation against the square root of time recorded during consolidation procedure at first loading of 50 kN/m^2 was plot as shown in Figure 4.8. Using Taylor's square root of time method, the square root of time at 90% consolidation was determined; at $\sqrt{t_{90}}$ = 9.05min

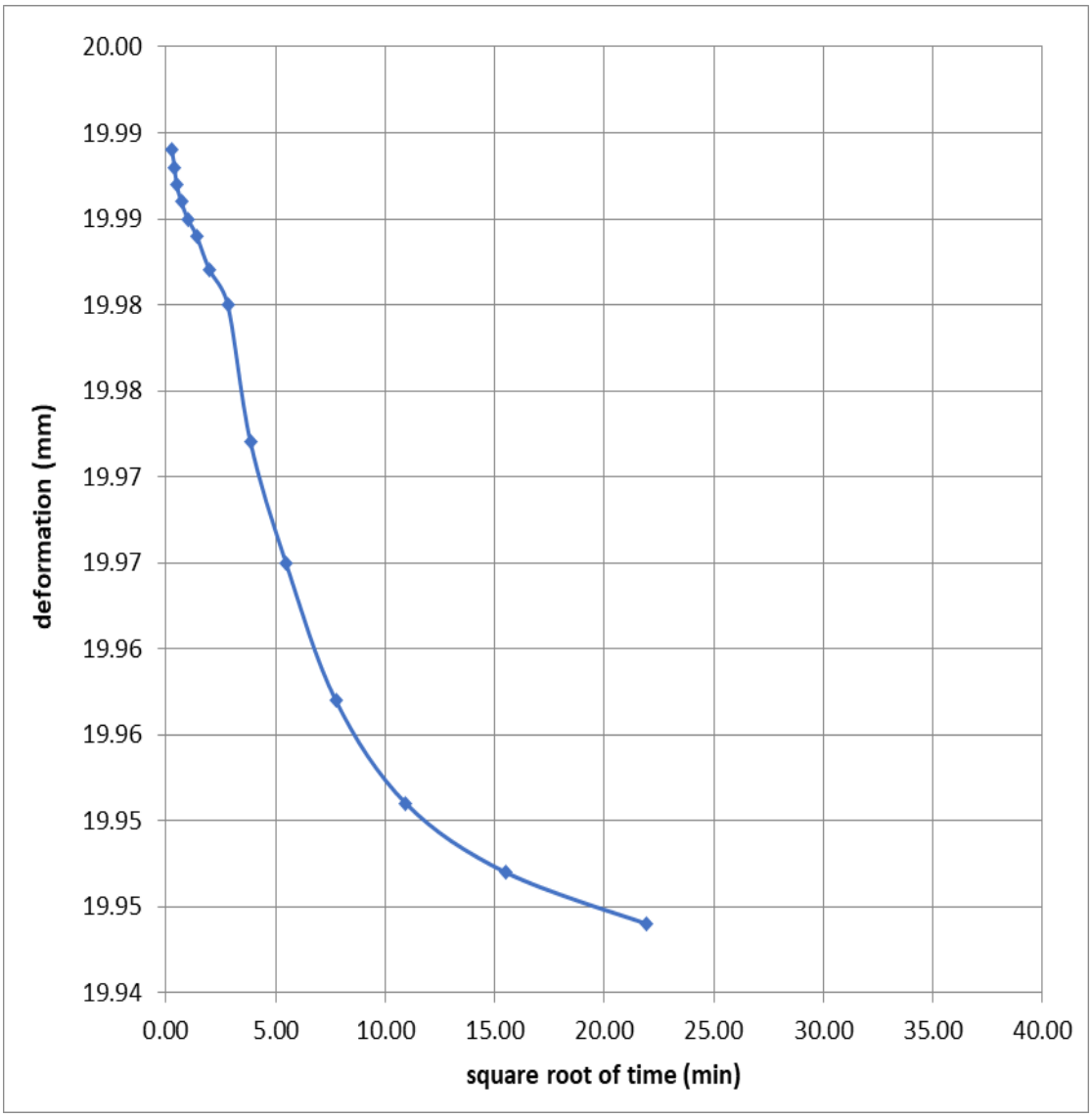

Figure 4.8: Deformation – Square root of time curve for 50 kN/m^2 ($\sqrt{t_{90}}$ = 9.05)

Graph of deformation against the square root of time recorded during consolidation procedure at first loading of 100 kN/m^2 was plot as shown in Figure 4.9. Using Taylor's square root of time method, the square root of time at 90% consolidation was determined; at $\sqrt{t_{90}}$ = 2.98min

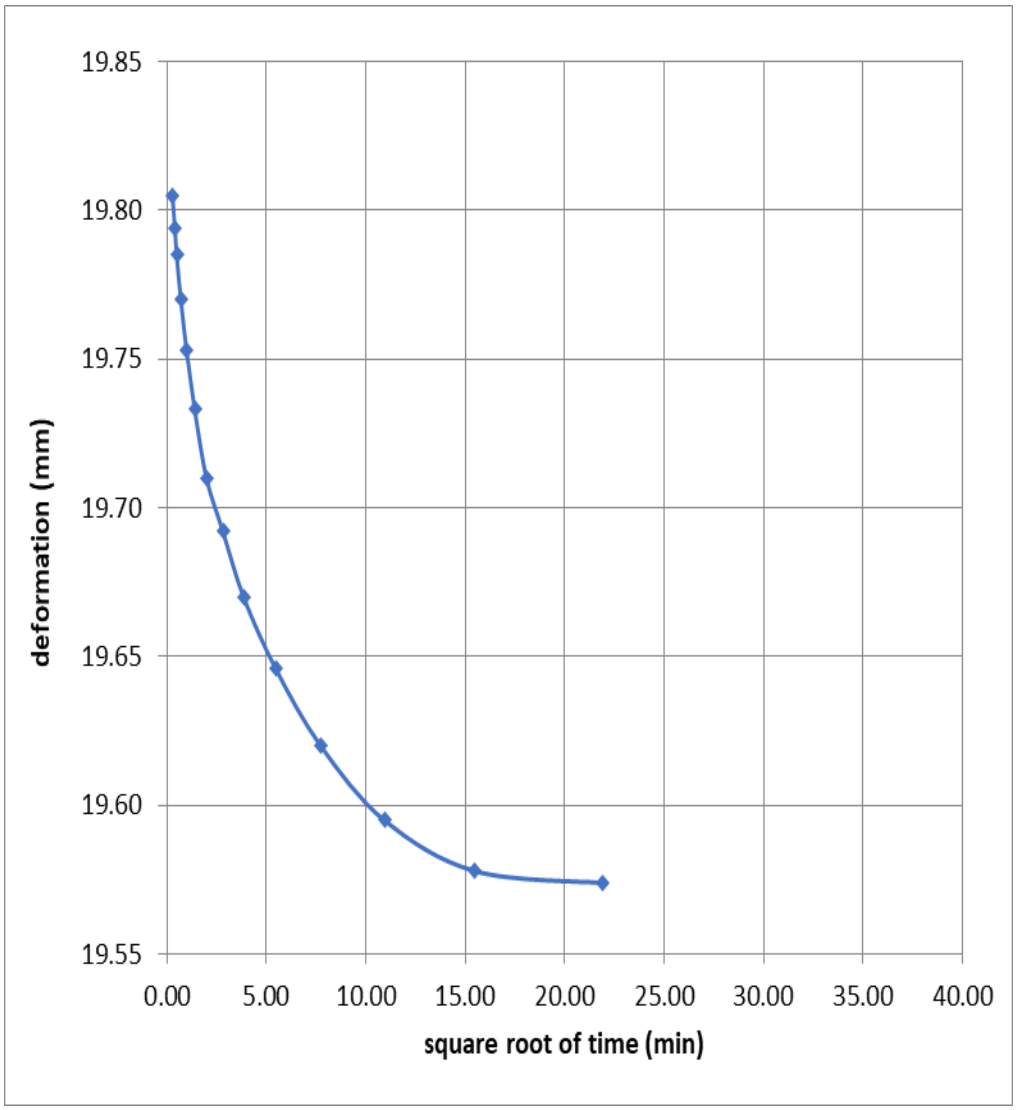

Figure 4.9: Deformation – Square root of time curve for 100 kN/m^2 ($\sqrt{t_{90}}$ = 2.98)

Graph of deformation against the square root of time recorded during consolidation procedure at first loading of 200 kN/m^2 was plot as shown in Figure 4.10. Using Taylor's square root of time method, the square root of time at 90% consolidation was determined; at $\sqrt{t_{90}}$ = 3.05min

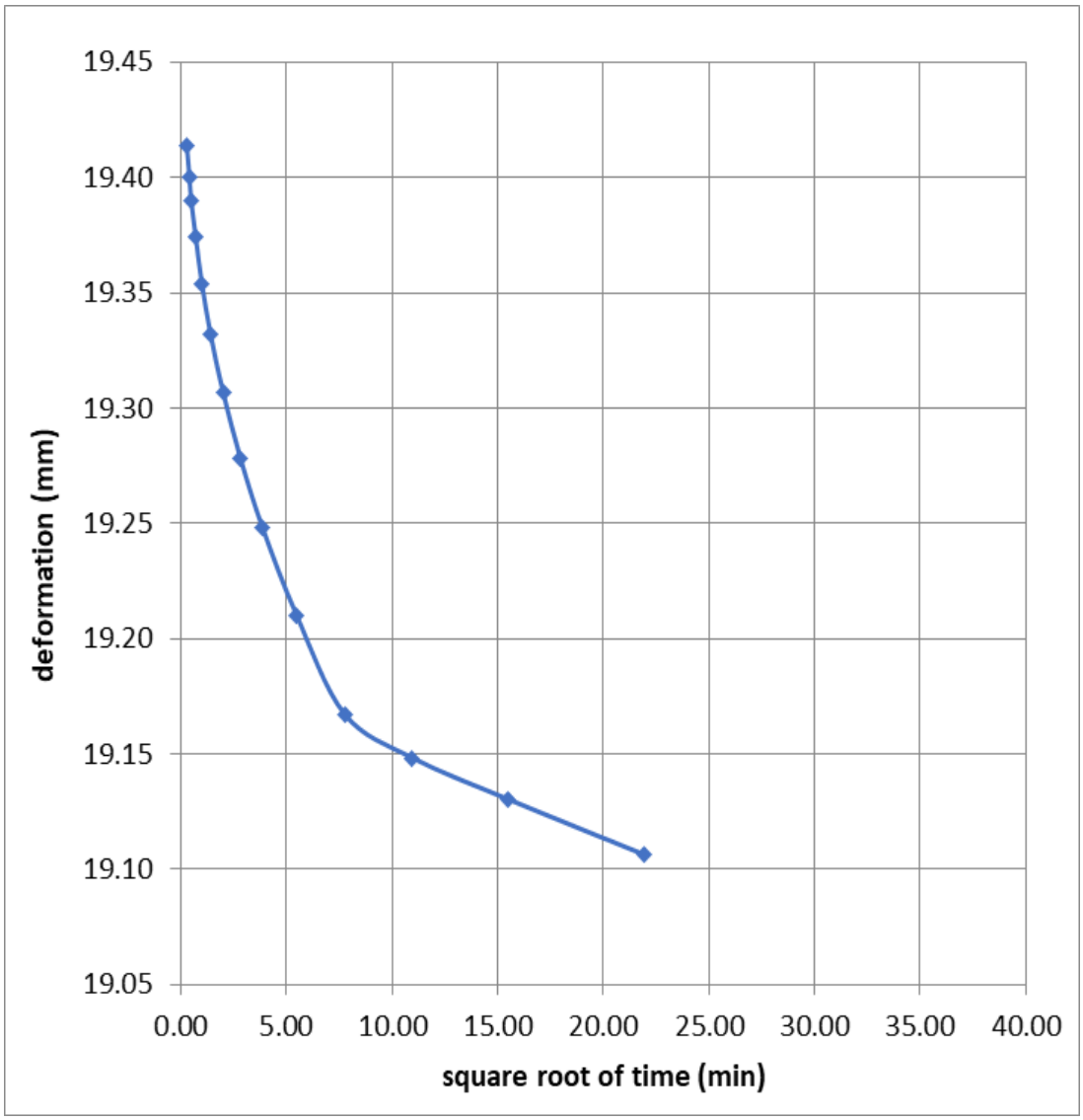

Figure 4.10: Deformation – Square root of time curve for 200 kN/m^2 ($\sqrt{t_{90}}$ = 3.05)

Graph of deformation against the square root of time recorded during consolidation procedure at first loading of 400 kN/m^2 was plot as shown in Figure 4.11. Using Taylor's square root of time method, the square root of time at 90% consolidation was determined; at $\sqrt{t_{90}}$ = 4.60min

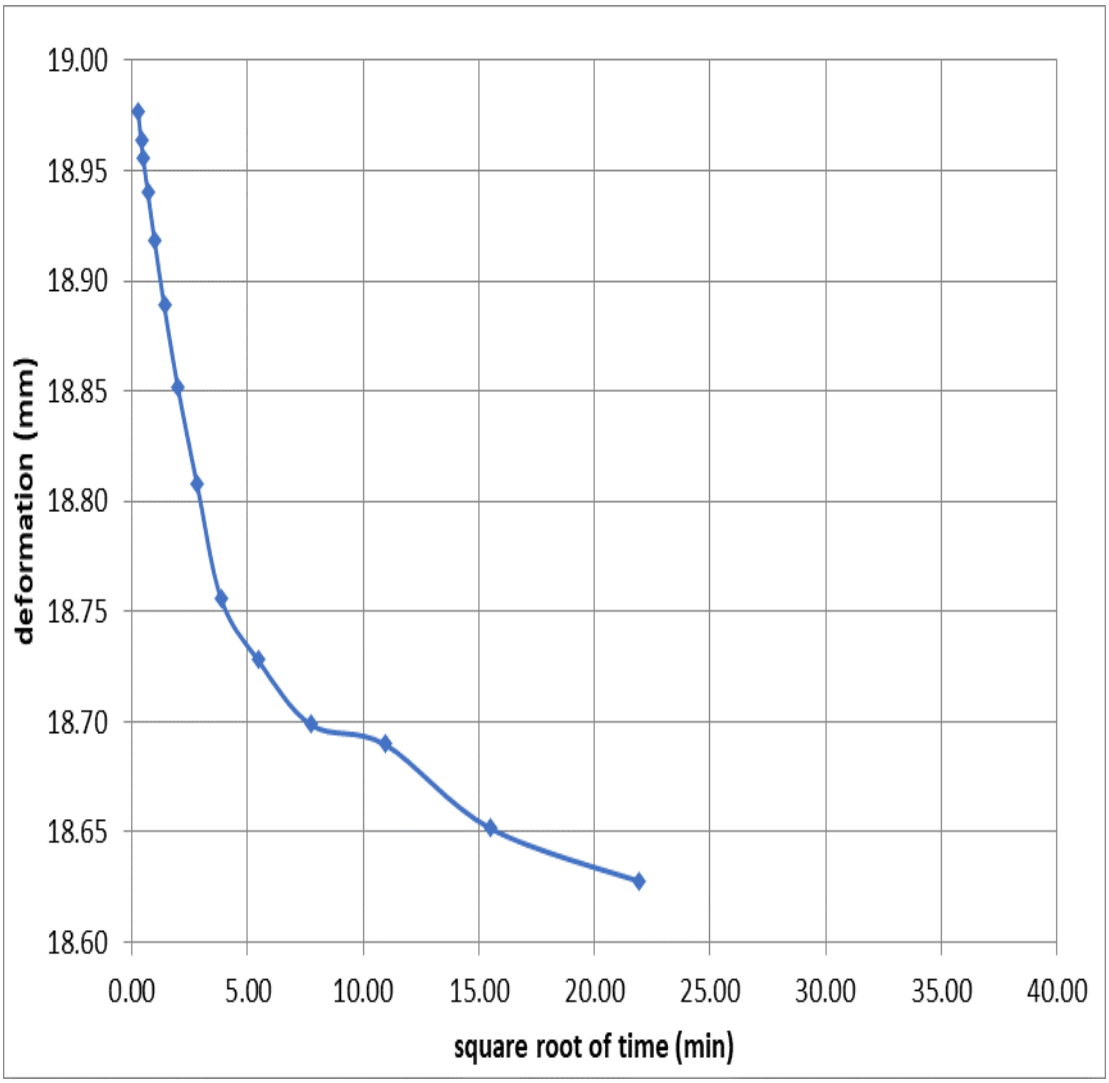

Figure 4.11: Deformation – Square root of time curve for 400 kN/m^2 ($\sqrt{t_{90}}$ = 4.60)

Graph of deformation against the square root of time recorded during consolidation procedure at first loading of 800 kN/m^2 was plot as shown in Figure 4.12. Using Taylor's square root of time method, the square root of time at 90% consolidation was determined; at $\sqrt{t_{90}}$ = 8.99min

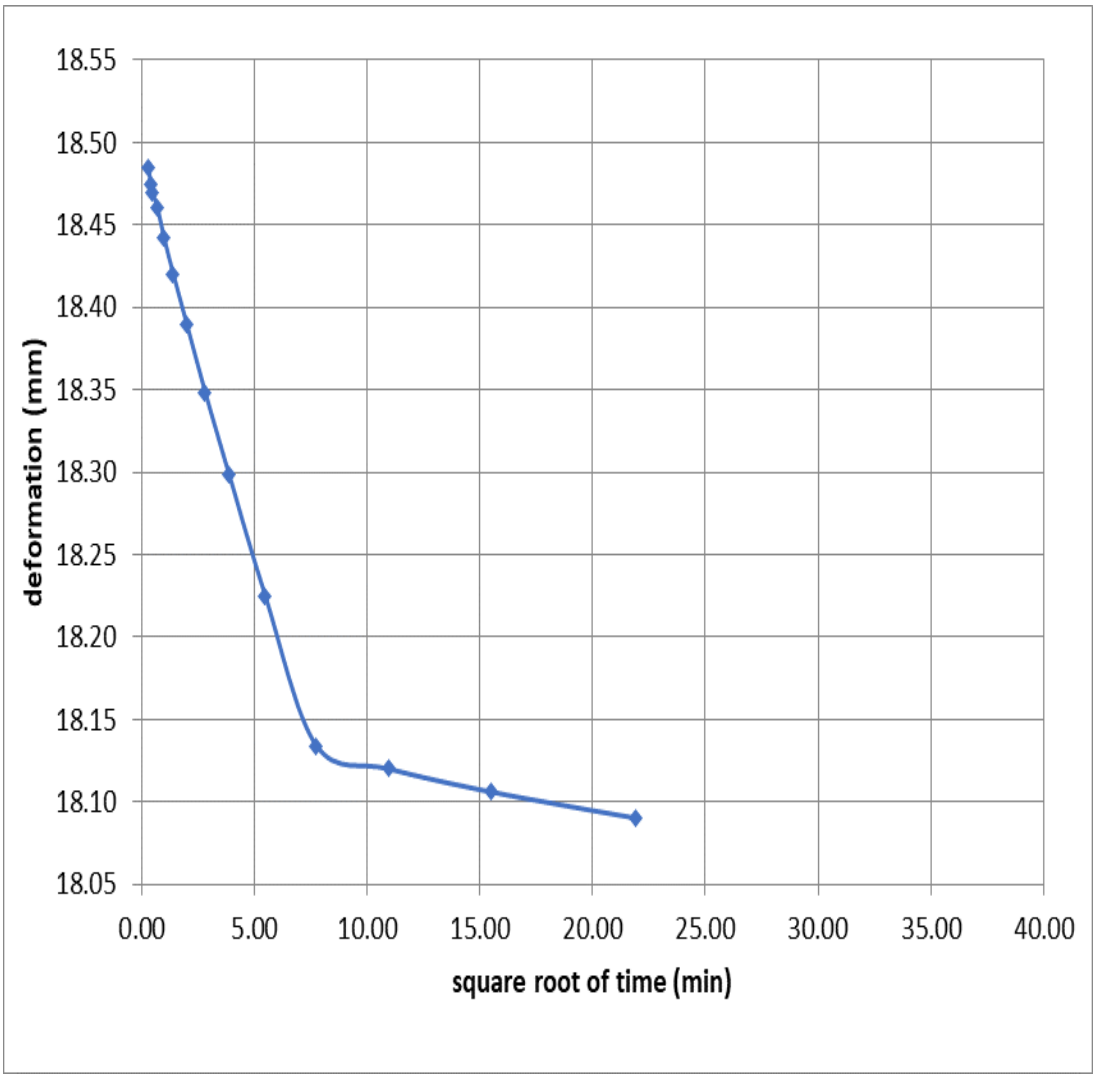

Figure 4.12: Deformation – Square root of time curve for 800 kN/m^2 ($\sqrt{t_{90}}$ = 8.99)

Graph of deformation against the square root of time recorded during consolidation procedure at first loading of 1600 kN/m^2 was plot as shown in Figure 4.13. Using Taylor's square root of time method, the square root of time at 90% consolidation was determined; at $\sqrt{t_{90}}$ = 11.40min

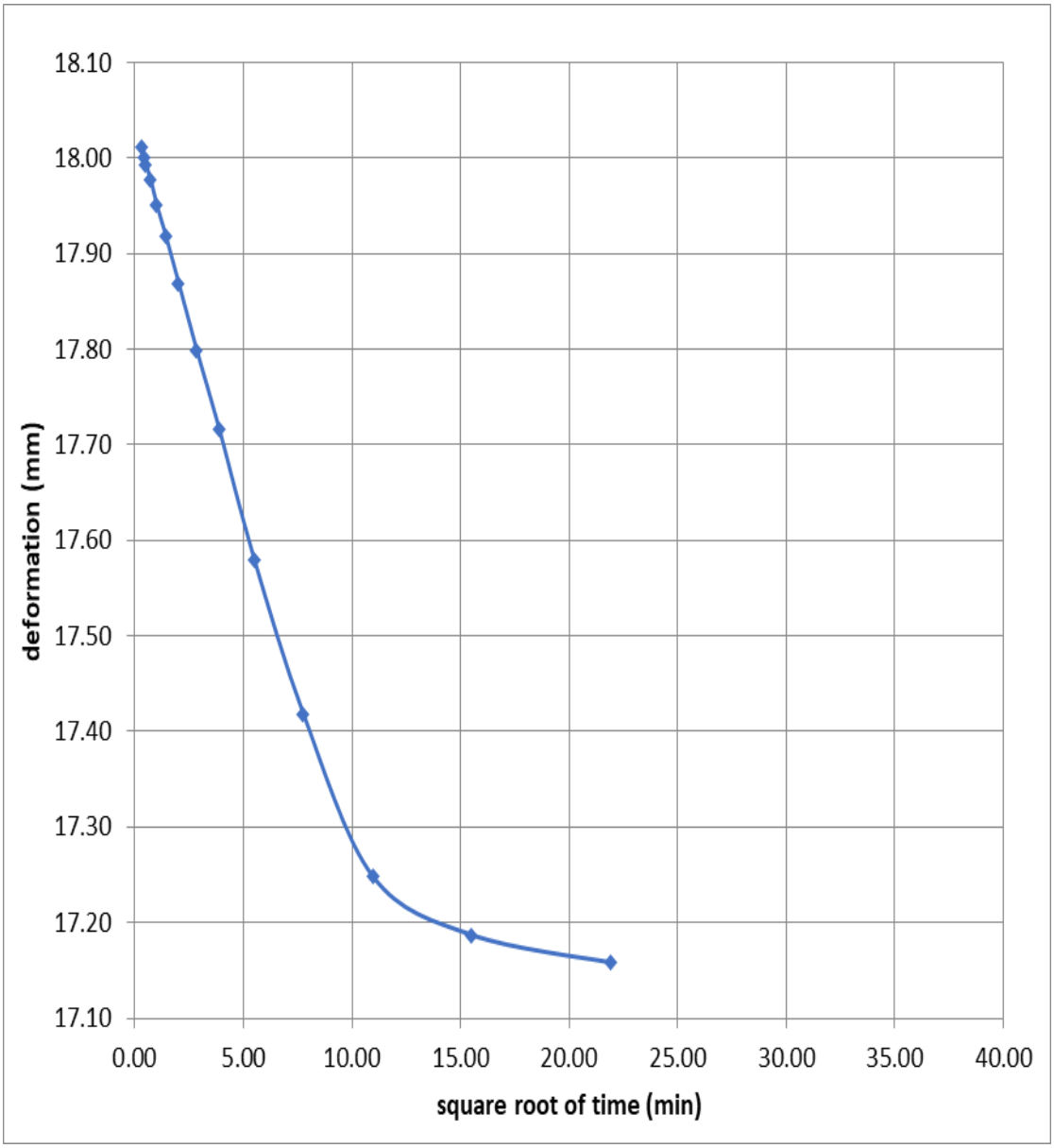

Figure 4.13: Deformation – Square root of time curve for 1600 kN/m^2 ($\sqrt{t_{90}}$ = 11.40

The value of t_{90} at 90% consolidation, U_{90} of each load increment were determined using Taylor's Square Root of time method as obtained from Figure 4.8 – 4.13.

The corresponding values of coefficient of consolidation c_{v1} for each load increment are analysed from the relationship $c_v = T_v d^2/t_{90}$ were $T_v = 0.848$ for U_{90} and presented in Table 4.6.

Table 4.6: Analysis of Consolidation Test Results – Sample 2

Applied pressure, σ (kN/m^2)	t_{90} (min)	Specimen height H (m)	Sample Depth $d^2 = (H/2)^2$ (m)	$c_v = 0.848d^2/t_{90}$ (m^2/min)
50	81.9025	0.0199	9.900E-05	1.025E-06
100	8.8804	0.0196	9.604E-05	9.171E-06
200	9.3025	0.0191	9.120E-05	8.314E-06
400	21.16	0.0186	8.649E-05	3.466E-06
800	80.8201	0.0181	8.190E-05	8.594E-07
1600	129.96	0.0171	7.310E-05	4.770E-07

From Table 4.6, the coefficient of consolidation ranges from 1.03 x 10^{-6} m^2/min to 9.1 x 10^{-6} m^2/min depending on the applied pressure. The weighted average coefficient of consolidation within the applied pressure is calculated as follows:

$C_{v2} = \frac{50}{1600} \text{x } 1.025 \text{ x } 10^{-6} + \frac{100}{1600} \text{x } 9.171 \text{ x } 10^{-6} + \frac{200}{1600} \text{x } 8.314 \text{ x } 10^{-6} + \frac{400}{1600} \text{x } 3.466 \text{x } 10^{-6} + \frac{800}{1600} \text{x } 8.594 \text{ x } 10^{-6}$

$C_{v2} = 3.203 \text{ x } 10^{-8} + 5.732 \text{ x } 10^{-7} + 1.039 \text{ x } 10^{-6} + 8.665 \text{ x } 10^{-7} + 4.297 \text{ x } 10^{-6}$

$C_{v2} = 6.808 \text{ x } 10^{-6} m^2/min$

4.2.2.1 *Void Ration of sample 2*

The final void ratio at the end of consolidation process is given by $e_f = mc_f \text{ x } G_s$

Given that, final moisture content mc_f, of the soil sample is 25%, final height H_f is 16.88mm and specific gravity G_s is 2.47 as obtained from the laboratory test.

Therefore,

$e_f = \frac{25.05}{100} \text{ x } 2.47$

$e_f = 0.619$

$\Delta e = \frac{1+e_f}{H_f} \text{ x } \Delta H$

$\Delta e = \frac{1+0.619}{17.452} \text{ x } \Delta H$

$\Delta e = 0.093 \Delta H$

The void ratios at each load increment was calculated and tabulated in Table 4.8. The graph of the relationship of void ratio – effective stress was plotted as shown in Figure 4.14.

Table 4.7: Void Ratio – Sample 2

Applied pressure, σ (kN/m^2)	Change in thickness ΔH (mm)	Specimen height H (mm)	Change in voids ratio Δe = 0.093ΔH	Voids ratio e
25		20		0.856
	-0.068		-0.006	
50		19.932		0.850
	-0.382		-0.036	
100		19.55		0.814
	-0.48		-0.045	
200		19.07		0.769
	-0.45		-0.042	
400		18.62		0.728
	-0.54		-0.050	
800		18.08		0.677
	-0.96		-0.089	
1600		17.12		0.588
	0.332		0.031	
12.5		17.452		0.619

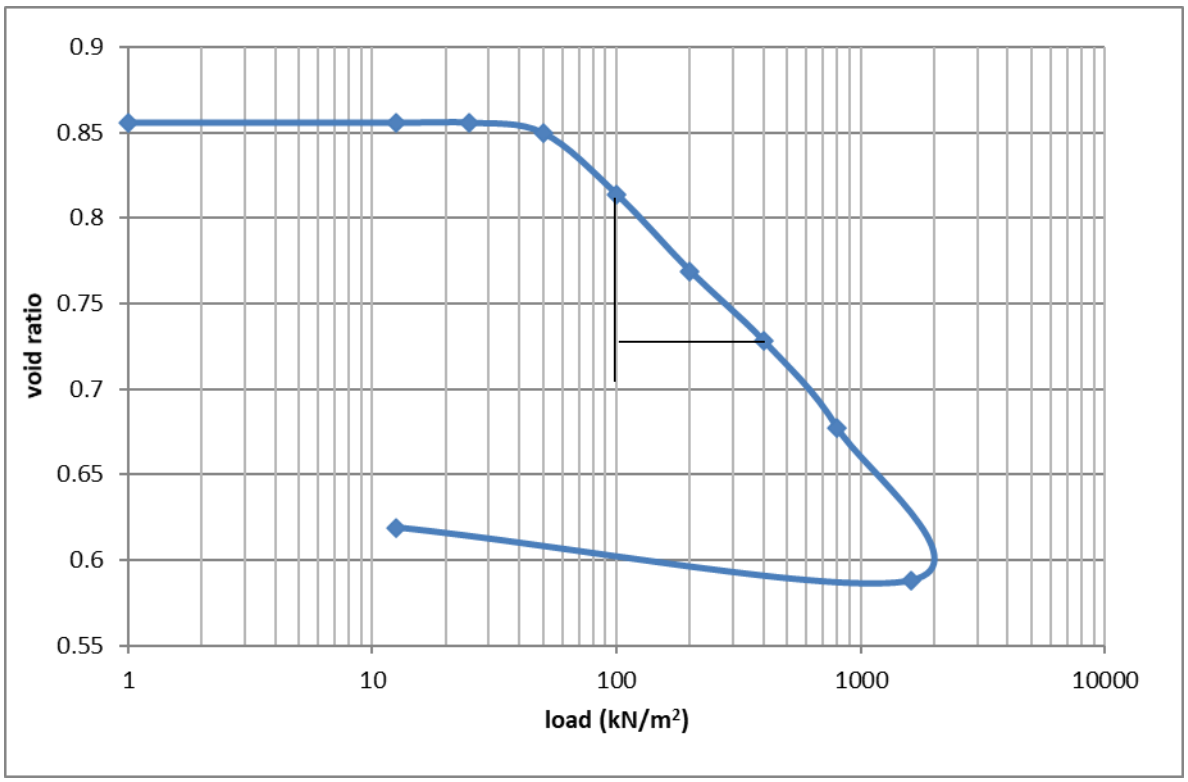

Figure 4.14: Void Ratio – Effective stress relationship

4.2.2.2 *Coefficient of compressibility of sample 2*

From Eq. 4.2, coefficient of compressibility m_{v2} is calculated thus;

$$m_{v2} = -\frac{\Delta e}{1+e_0} \text{ x } \frac{1}{\Delta \sigma}$$

$$m_{v2} = -\frac{0.814-0.728}{1+0.728} \frac{1}{400-100} = \frac{0.086}{1.728} \text{ X } \frac{1}{300}$$

$$m_{v2} = 1.659 \text{ x } 10^{-4} \text{ m}^2/\text{kN}$$

4.2.2.3 *Coefficient of permeability of sample 2*

$$k_2 = c_{v2} \text{ x } m_{v2} \text{ x } \gamma_w$$

$$k_2 = 6.808 \text{ x } 10^{-6} \text{ x } 1.659 \text{ x } 10^{-4} \text{ x } 9.81$$

$$k_2 = 1.11 \text{ x } 10^{-8} \text{m/min}$$

The summary of consolidation properties of the two clayey soil used for this study were presented in Table 4.8

Table 4.8: Summary of Consolidation Properties

	Cv (m^2/min) x 10^{-6}	Mv (m^2/kN) x 10^{-4}	K (m/min) x 10^{-8}
Sample 1	5.466	3.053	1.64
Sample 2	6.808	1.659	1.11

4.3 Model Validation

4.3.1 Variation of excess pore pressure of single layer (sample 1)

The variation of excess pore water pressure u with depth z at different time t for a single layer clayey soil element was presented in Figure 4.15

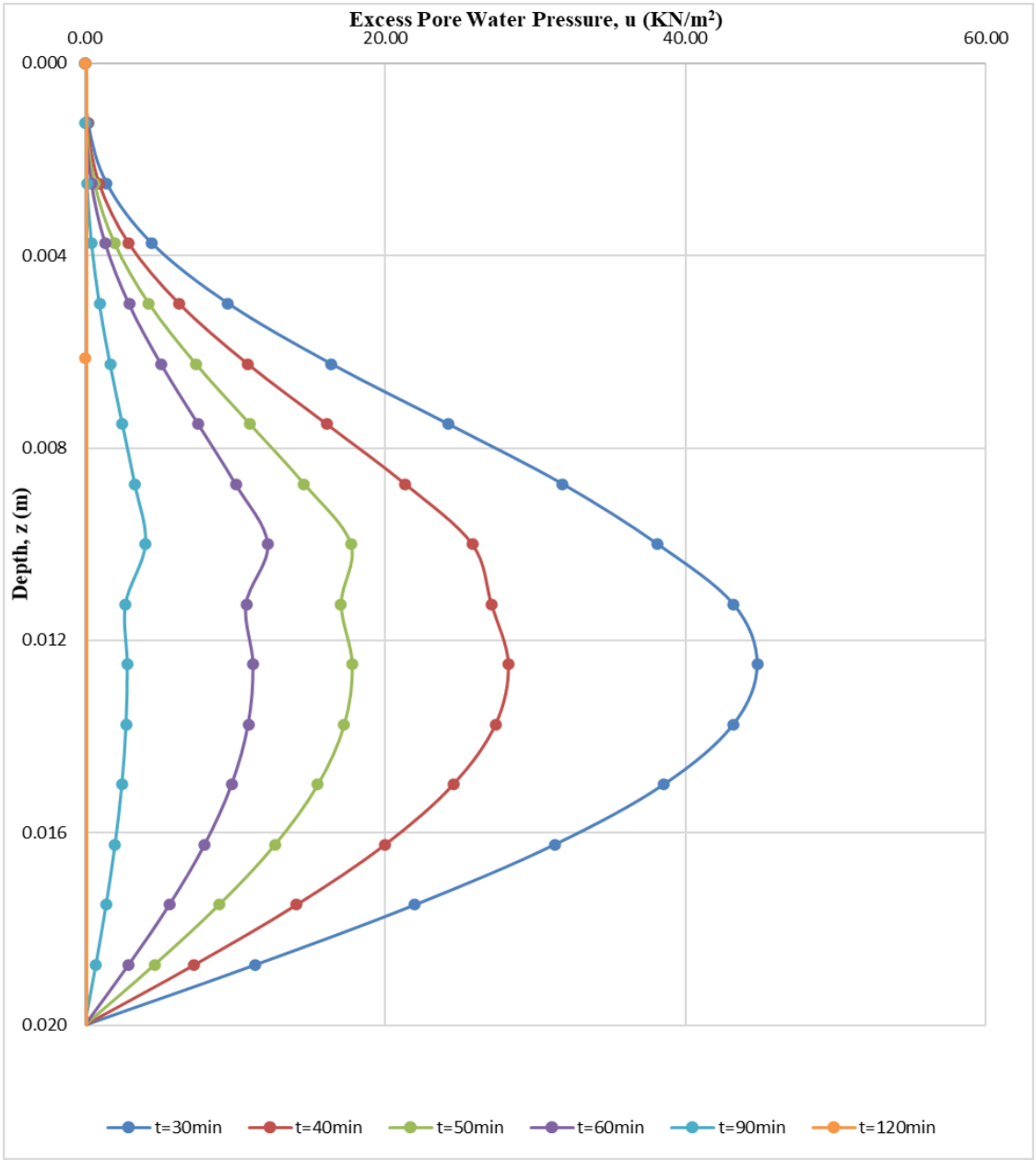

Figure 4.15: Variation excess pore pressure of sample 1

4.3.2 Variation of excess pore pressure of single layer (sample 2)

The variation of excess pore water pressure u with depth z at different time t for a single layer clayey soil element was presented in Figure 4.16

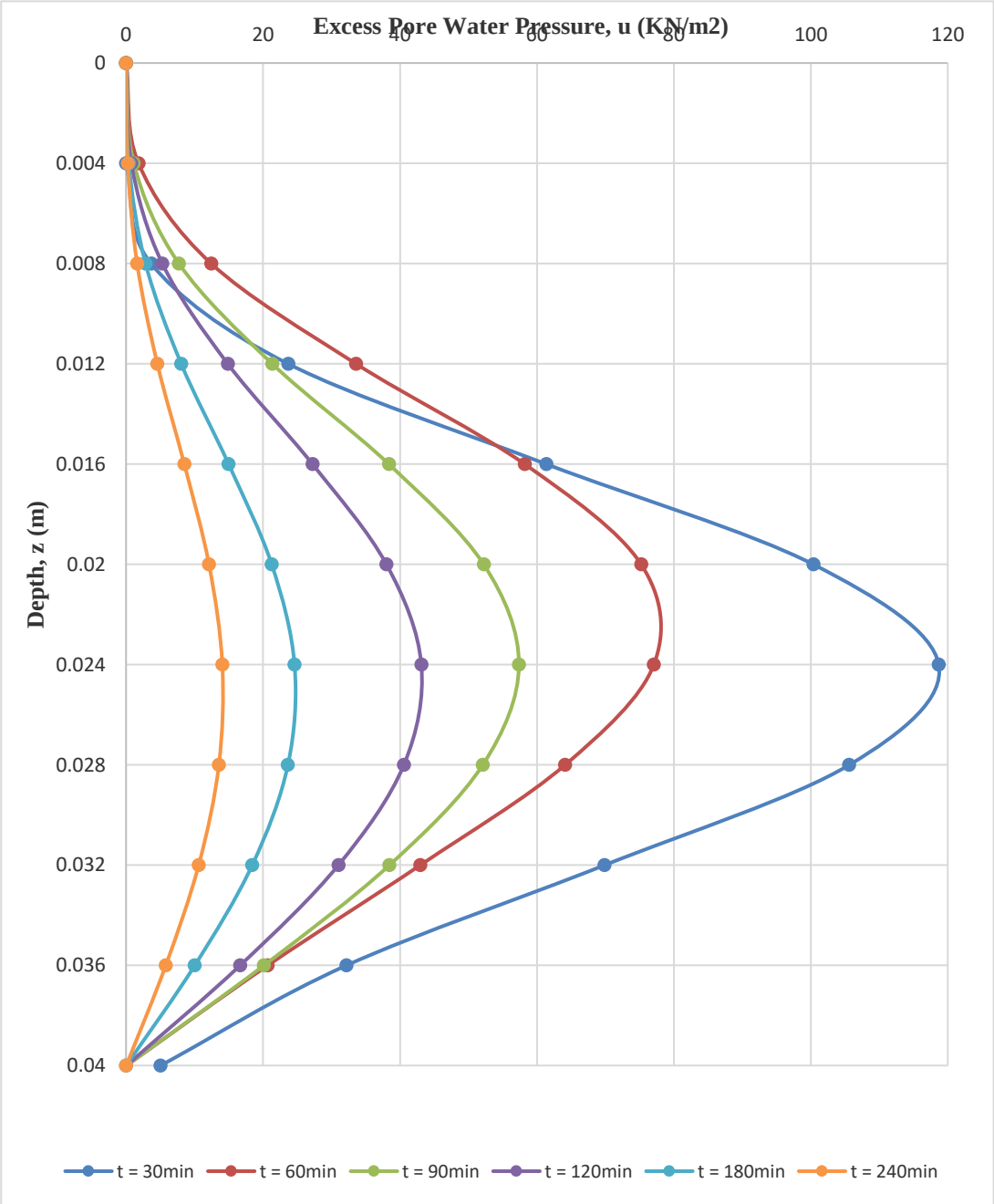

Figure 4.16: Variation of excess pore pressure of sample 2

4.3.3 Variation of excess pore pressure of double layer

The theoretical variation of excess pore water pressure u with depth z at different time t for double layer clayey soil element determine from Eq. 3.10, 3.11 and 3.12 and presented in Figure 4.17

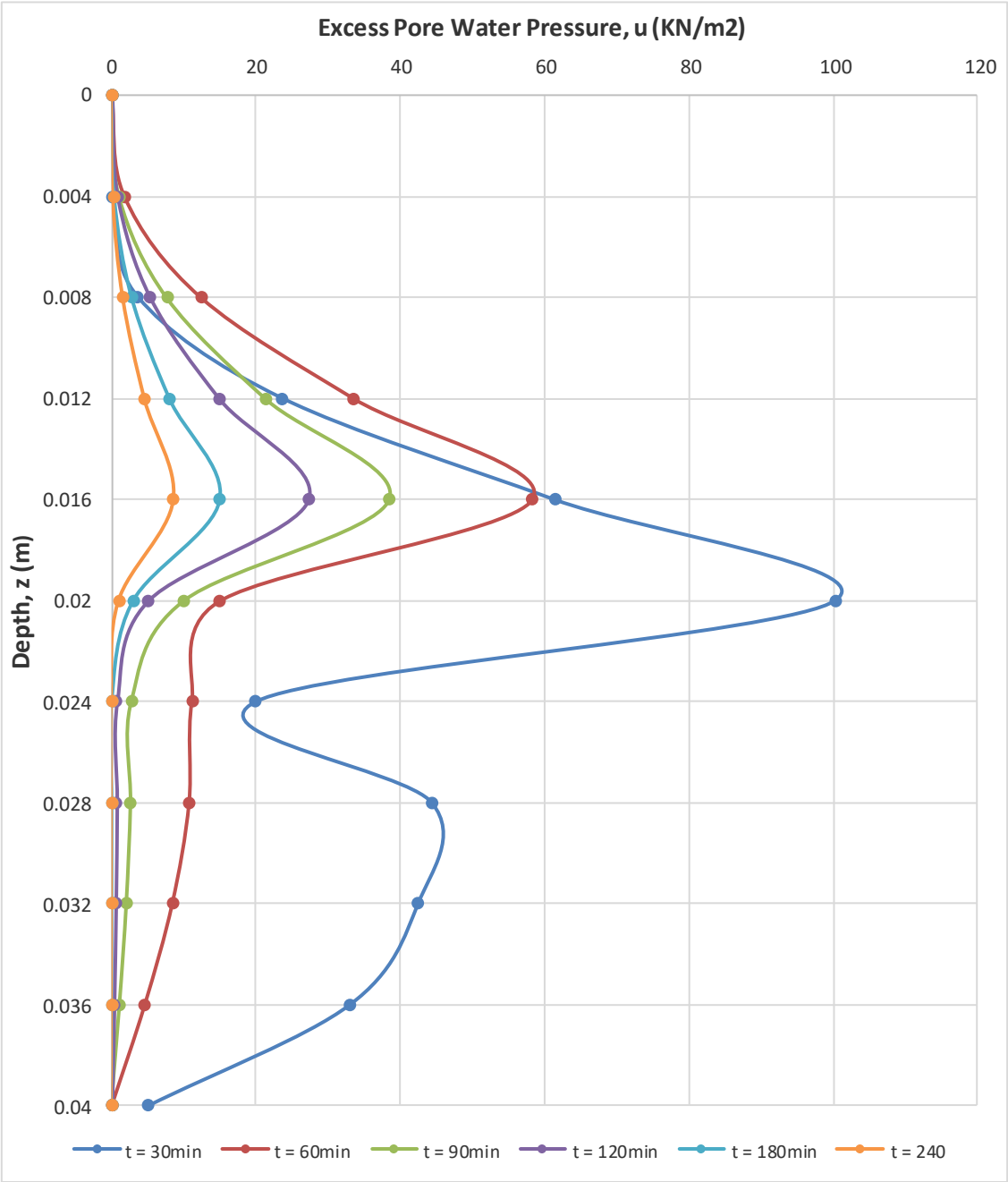

Figure 4.17: Variation of excess pore water pressure of double layered

4.3.4 Degree of consolidation

Table 4.9 shows the theoretical and laboratory degree of consolidation of both soil samples in relation to square root of time. The relationship of the two is plotted in Figure 4.20

Table 4.9: Corresponding Value of U with Time

Square Root of Time	Sample 1 Theoretical U	Sample 2 Theoretical U	Sample 1 laboratory U	Sample 2 laboratory U
0.29	0.068	0.076	0	0
0.41	0.068	0.084	0.135	0.032
0.5	0.068	0.091	0.202	0.054
0.71	0.069	0.111	0.281	0.095
1	0.071	0.143	0.393	0.147
1.41	0.074	0.189	0.472	0.202
2	0.08	0.254	0.584	0.26
2.83	0.092	0.357	0.596	0.326
3.87	0.11	0.517	0.663	0.379
5.48	0.143	0.765	0.73	0.44
7.75	0.191	0.952	0.787	0.503
10.95	0.259	0.998	0.854	0.557
15.49	0.362	1	0.899	0.609
21.91	0.534	1	0.944	0.713
30.98	0.669	1	0.978	0.826
37.94	0.893	1	1	1

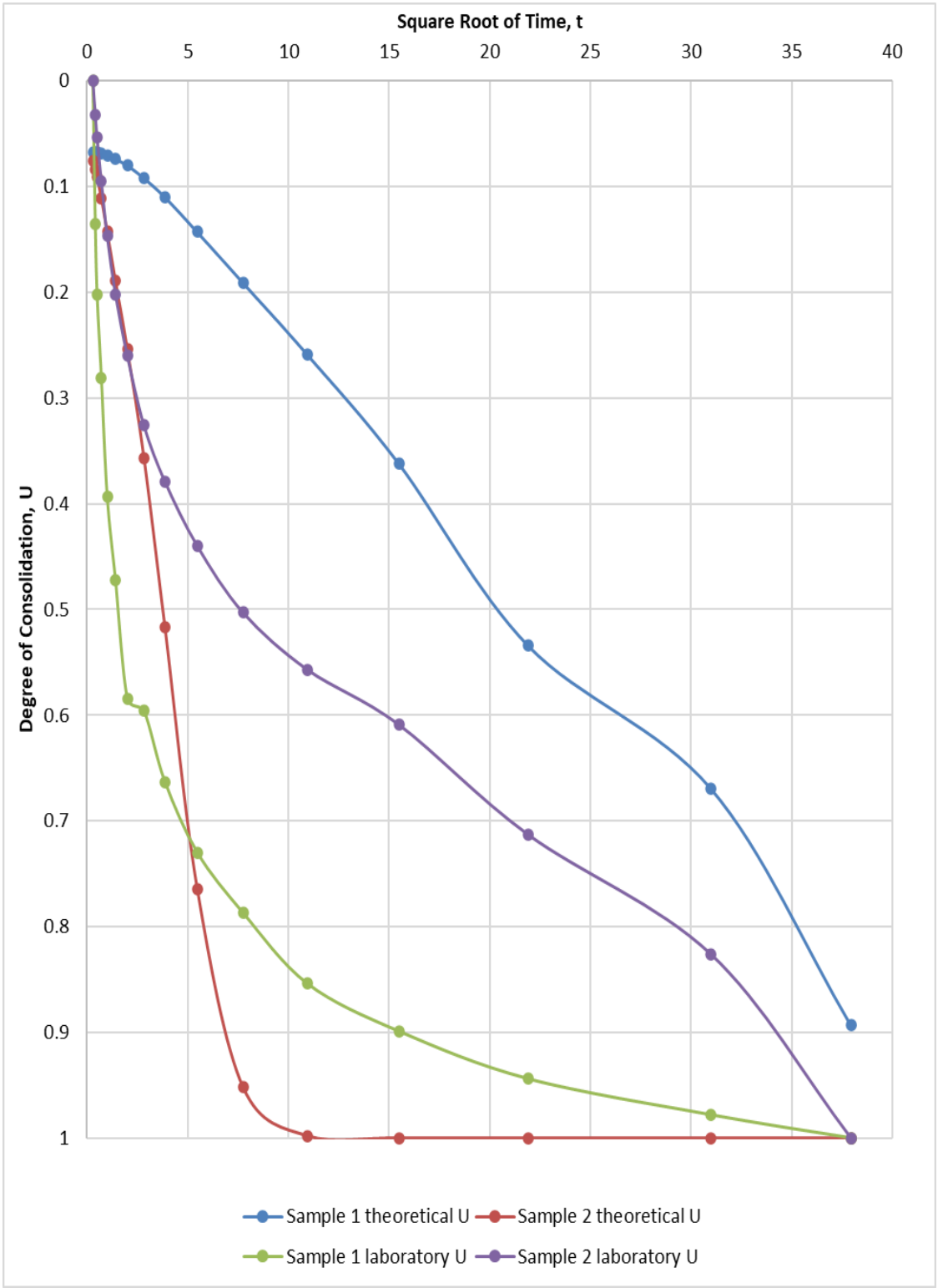

Figure 4.18: Degree of consolidation – square root of time relationship

The theoretical degree of consolidation and the laboratory degree of consolidation of the two soil samples are calculate based on Eq. 2.39. The relationship of the two is shown in Figure 4.20. The proposed analytical model shows a significant variation from the laboratory analysis for sample 1 in terms of rate of consolidation at any given time. The theoretical analysis of sample 2 show some similarities with the laboratory analysis as an indication of the realistic of the proposed analytical model.

CHAPTER FIVE

5.0 CONCLUSION AND RECOMMENDATIONS

5.1 Conclusion

The generated index properties of the clayey soil sample show that the soil sample used for this research work is classified as clayey material based on AASHTO standard of classification. Hence not suitable for road construction and should be treated as cut to spoil or stabilised where its usage is unavoidable.

The consolidation coefficient generated using Taylor's square root of time method under various loading application at different time interval was used to calculate the compressibility and permeability coefficient.

The analytical model under review is validated in terms of the variation of excess pore water pressure distribution in the soil samples as presented in Figure 4.17 which show a significant conformity as compared with Figure 8.7 (Braja, 2019) and Figure 11 (Herrmann and El Gendy, 2014) of excess pore water pressure variation with depth for double-layered clayey soil. The comparison shows a good agreement and this is an indication that the proposed analytical solution for double-layered soil as presented by Sadiku is in line with other scholars.

5.2 Recommendations

This research creates the opportunity for future works by widening the scope to increase its acceptability. Some of the recommendations for future work are listed below:

1. The study is to validate analytical model under review. A further verification in terms of in-situ test will increase the acceptability of the model.

2. Further study for lateral drainage condition for multi-dimensional model can be established
3. Road failure due to settlement and soil expansibility will be eliminate if this procedure is incorporated into the routine test for road construction in the construction industry, thereby saving life and properties.

5.3 Contribution to Knowledge

This study has further enhanced the validation of the proposed analytical model for the variation of excess pore water pressure of one-dimensional consolidation of double layered clayey soil thus, adding to its credibility and acceptability.

REFERENCES

Arnold, V. (2004). Soil Mechanics. Delft University of Technology, 84 – 110.

AASHTO. (2021). Standard Specifications for Transportation Material and Method of Sampling and Testing. Forty-one Edition, American association of State Highway and transportation officials.

Braja M.D. (2019). Advance Soil Mechanics. Fifth Edition, Taylor & Francis, 6000 Broken Sound Parkway NW, Suite 300 Boca Raton, FL 33487-2742.

Braja, M.D. (1997). Advance Soil Mechanics. Second edition, Taylor & Francis, 1101 Vermont Avenue, NW, Suite 200 Washington, DC. 20005-3521.

British Standard BS: 1377 (1990). Methods of Test of Soil for Civil Engineering Purposes. Section 2.7

Davis, E.H. & Raymond, G.P. (1965). A nonlinear theory of consolidation. Geo-technique. 15, 161 – 173.

Guofu, Z. & Jian-Hau, Y. (2000). Finite Element Consolidation Analysis of Soils with Vertical Drain. *International Journal for Numerical and Analytical Method in Hermethanics.* 24(4), 337-366.

Herrmann, R., & El Gendy, M. (2014). A layer equation method for 1-D consolidation under time-Dependent Reloading. *Ain Shams Engineering Journal.* 5, 1043–1057.

Junhui, Z., Guangming, C., Weizheng, L., & Houxuan, W. (2015). One-Dimensional Consolidation of Double-layered Foundation with Depth-Dependent Initial Excess *Pore* Pressure. *Advances in Materials Science and Engineering.*

Kang-He, X., Xi-Yu, X. & Wen, J. (2002). A study on one-dimensional nonlinear consolidation of double-layered soil. Computer and Geotechnics, Institute of geotechnical engineering, Zhejiang University, Hangzhou, 310027, PR China, 29(2002), 151- 168.

Kim, P., Kim, H., Pak, C., Paek, C., Ri, G. & Myong, H. (2021). Analytical Solution for One-Dimensional Nonlinear Consolidation of Saturated Multi-Layered Soil under Time-Dependent Loading. *Journal of Ocean Engineering and Science.* 6(1) 21-29.

Linchang, M., Xinhui, W., & Edward, K. Jr. (2008). Consolidation of a Double-Layered Compressible Foundation Partially Penetrated by Deep Mixed

Column. *Journal of Geotechnical and Geo-environmental Engineering.* 134:1210-1214.

Miao, L., Wang X & Kavazanjian, E. Jr (2008). Consolidation of a Double-Layered Compressible Foundation Partially Penetrated by Deep Mixed Columns. *Journal of Geotechnical and Geo-environmental Engineering.* 134(8), 1210 – 1214.

Murthy, V.N.S (2007). Soil Mechanics and Foundation Engineering. First Edition, Geotechnical Series CBS Publisher Ltd, New Delhi – 110002 India, 305-311.

Olson, R.E. (1977). Consolidation under Time Dependent Loading. *Journal of the Geotechinal Engineering Division*. 103(1) 1977.

Sadiku, S. (1991). Analytical and Computational Studies on the Consolidation of multi-layered soils. *Engineering Computation,* 8, 181-188.

Sadiku, S. (2013). Analytical and Computational Procedure for solving the consolidation problem of layered soils. *International Journal for Numerical and Analytical Methods in Geomechanics,* 37(16), 2789-2800.

Schiffman, R. & Stein, J.R. (1970). One-Dimensional Consolidation of Layered Systems. *Journal of the Mechanics and Foundation Division,* 96, 1499 – 1504.

Singh, A. (2002) Soil engineering in theory and practice. Fourth edition, Satish Kumar Jain, 4596/1-A, 11 Darya Ganj, New Delhi-110 002 (India). 1, 242 – 299.

Skempton, A. & Bjerrum, L. (1957). A Contribution to the Settlement Analysis of Foundation on Clay. *Journal for Geotechnics,* 7, 168 – 178.

Smith, M.J. (1981). Soil Mechanics. Longman Scientific and Technical, Longman group UK Ltd, Longman House, Burnt Mill, Harlon, Fourth Edition 64-75.

Suhua, Z., Jiatao, K., Chang, L., Minghua, H. (2021). One-Dimensional Consolidation of Multi-Layered Unsaturated Soil with Impeded Drainage Boundaries. *Applied Sciences*, 11(1), 2076-3417.

Tawfek S. A. (2017). Study of the Excess Pore Water Pressure in two Different Clay Soil Layers. *International Journal of Trend in Research and Development, 3(5), ISSN: 2394-9333*

Terzaghi, K. (1925). Principles of Soil Mechanics: I – Phenomena of Cohesion of Clays. *Engineering News-Record,* 95(19), 742-746.

Terzaghi, K. (1943). Theoretical Soil Mechanics, John Wiley and Sons, New York ISBN 0-471-85305-4.

Wenbing, W., Mengfan, Z., Mhesham, E., Guoxiong, M. & Rongzhu, L. (2018). Analytical Solution for One-Dimensional Consolidation of Double-Layered Soil with Exponentially Time-Growing Drainage Boundary. *International Journal of Distributed Sensor Networks*. 14 (10).

Tang, X. & Onitsuka, K. (2001). Consolidation of double-layered ground with vertical drains. *International Journal for Numerical and Analytical Methods in Geomechanics*, 25(14), 1449-1465.

Zhou, T., Wang, L., Li, T., Wen, M. & Zhou, A. (2023). Semi-analytical Solution to the One-dimensional Consolidation for double-layered unsaturated ground with a horizontal drainage layer. *Journal of Transportation Geotechnics*. https://doi.org/10.1016/j.trgeo.2022.100909

Zhao, X., Liu, Y. & Gong, W. (2020). Analytical Solution for One-dimensional Electro-osmotic Consolidation of double layered system. *Journal of Computer and Geotechnics*. https://doi.org/10.1016/j.compgeo.2020.103496

Zhuang, Y., Xie, K. & Li-bin. (2005). Nonlinear Analysis of Consolidation with variables Compressibility and permeability. *Journal of Zhejiang University Science*. ISSN 1009-3095, 6A (3), 181-187.

APPENDICES

APPENDIX A

Table A1: Specific Gravity Sample 1

Sample: Clayey Soil at 1.5m Depth		1	2	3
Container No.				
Mass of clay soil + bottle (m_2)	(g)	102.40	105.97	105.70
Mass of clay soil + bottle + water (m_3)	(g)	187.49	191.04	191.99
Mass of empty bottle (m_1)	(g)	65.99	70.53	73.13
Mass of bottle + water (m_4)	(g)	164.63	169.03	172.28
Specific Gravity, $Gs = \frac{(m_2 - m_1)}{(m_4 - m_1) - (m_3 - m_2)}$		2.69	2.64	2.53
		Average Gs = 2.62		

Table A2: Specific Gravity Sample 2

Sample: Clayey Soil at 1.5m Depth		1	2	3
Container No.				
Mass of clay soil + bottle (m_2)	(g)	97.97	99.14	72.93
Mass of clay soil + bottle + water (m_3)	(g)	187.11	186.55	162.41
Mass of empty bottle (m_1)	(g)	73.04	70.62	48.61
Mass of bottle + water (m_4)	(g)	172.31	169.37	148.06
Specific Gravity, $Gs = \frac{(m_2 - m_1)}{(m_4 - m_1) - (m_3 - m)}$		2.46	2.51	2.44
		Average Gs = 2.47		

Table A3: Liquid and Plastic Limit Sample 1

	LIQUID LIMIT					PLASTIC LIMIT	
Can Number	1	2	3	4	5	1	2
Penetration	2.5	7.2	14.2	18.2	22.2		
Can Weight	35.97	37.55	36.9	37.3	35.41	36.96	37.62
Can Weight + Wet Soil	43.52	51.63	56.17	60.02	61.24	44.44	45.25
Can Weight + Dry Soil	42.27	48.57	51.05	53.67	53.59	43.27	44.01
Weight of Moisture	1.25	3.06	5.12	6.35	7.65	1.17	1.24
Weight of Dry Soil	6.3	11.02	14.15	16.37	18.18	6.31	6.39
Moisture Content	19.84	27.77	36.18	38.79	42.08	18.54	19.41
Liquid Limit	41.09%		Average Plastic Limit			18.97%	

Table A4: Liquid and Plastic Limit Sample 2

	LIQUID LIMIT					PLASTIC LIMIT	
Can Number	1	2	3	4	5	1	2
Penetration	6.8	10.1	14	20.4	24.1		
Can Weight	37.51	37.54	35.64	37.5	37.79	36.93	36.89
Can Weight + Wet Soil	51.38	57.1	58.17	60.34	62.08	46.15	45.36
Can Weight + Dry Soil	48	52	5187	53.61	54.68	44.12	43.49
Weight of Moisture	3.38	5.1	6.3	6.73	7.4	2.03	1.87
Weight of Dry Soil	10.49	14.46	16.23	16.11	16.89	7.19	6.6
Moisture Content	32.22	35.27	38.82	41.78	43.81	28.23	28.33
Liquid Limit	41.66%		Average Plastic Limit			28.28%	

Table A5: Grain Size Analysis Sample 1

Weight of Sample 300g

Sieve size (mm)	Mass retained (g)	% Retained	% Passing
5.000	0.00	0.00	100.00
3.350	0.00	0.00	100.00
2.000	1.00	0.33	99.67
1.180	8.10	2.70	96.97
0.850	12.00	4.00	92.97
0.600	20.10	6.70	86.27
0.425	29.30	9.77	76.50
0.300	19.40	6.47	70.03
0.150	28.30	9.43	60.60
0.075	15.20	5.07	55.53

Table A6: Grain Size Analysis Sample 2

Weight of Sample 300g

Sieve size (mm)	Mass retained (g)	% Retained	% Passing
5.000	0.70	0.23	99.77
3.350	0.50	0.17	99.60
2.000	2.40	0.80	98.80
1.180	2.70	0.90	97.90
0.850	2.30	0.77	97.13
0.600	3.70	1.23	95.90
0.425	6.80	2.27	93.63
0.300	10.10	3.37	90.27
0.150	34.90	11.63	78.63
0.075	38.80	12.93	65.70

APPENDIX B

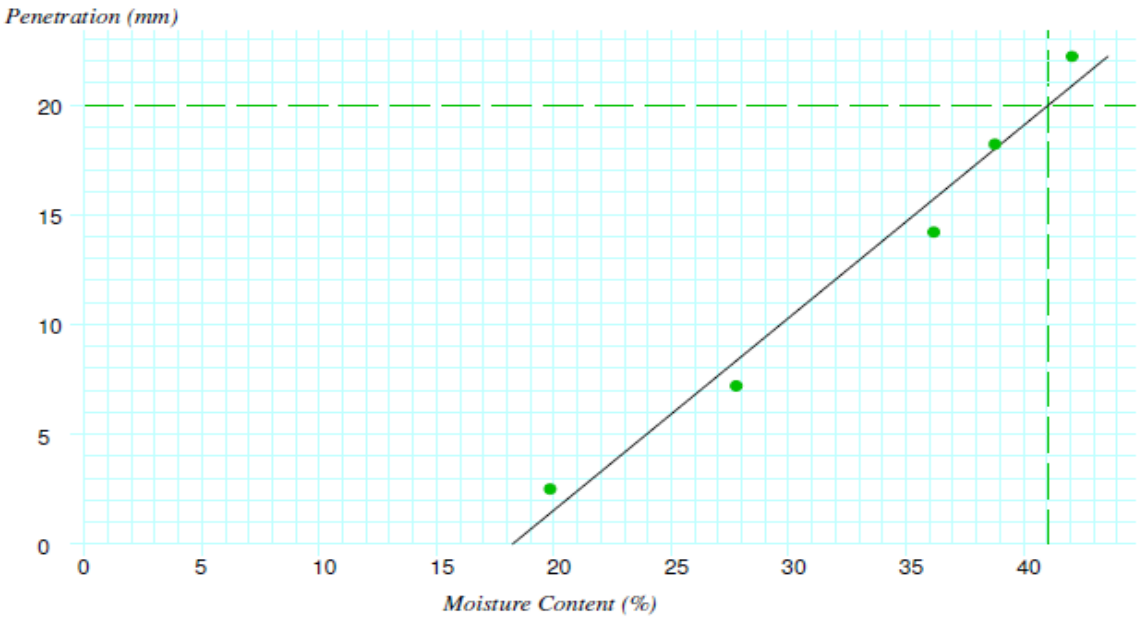

Figure B1: Penetration – Moisture Content Relationship Sample 1

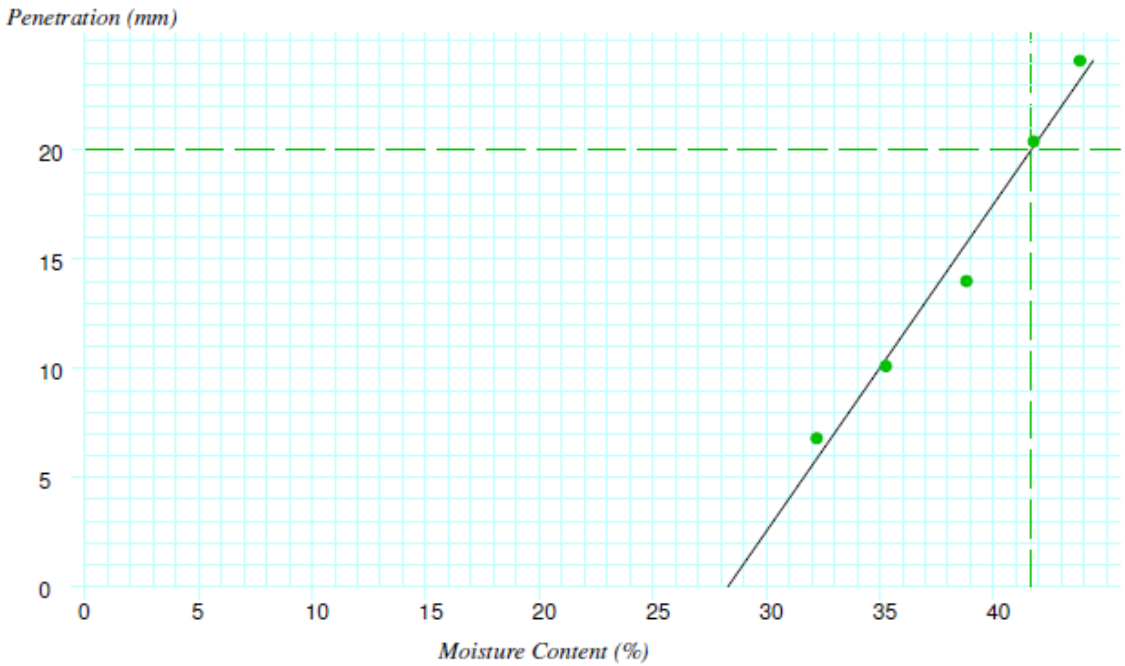

Figure B2: Penetration – Moisture Content Relationship Sample 2

APPENDIX C

Plate I: Soil Sample Collection

Plate II: Soil Sample Collection

Plate III: Soil Sample 1

Plate IV: Soil Sample 2

Plate V: Consolidation Apparatus

Plate VI: Double Layered Consolidation

Plate VII: Cone Penetration Test Apparatus

Plate VIII: Fabricated Consolidation Mould and Ring